2023

kunanyi/Mount Wellington debris flow susceptibility and hazard assessment

Author: C. Mazengarb, T. Rigby and M. Stevenson
Date: 05/07/2023
Email: info@mrt.tas.gov.au
Website: www.mrt.tas.gov.au

REPORT No.: TR37

Geological Survey Technical Report 37

Tasmanian Government

Mineral Resources Tasmania
Department of State Growth

Geological Survey Technical Report 37:

kunanyi/Mount Wellington debris flow susceptibility and hazard assessment

by C. Mazengarb, T. Rigby and M. Stevenson

Cover: Debris flow at Newtown Rivulet, triggered by a rainstorm event in May 2018.

Definition

Debris flows (sensu lato), as paraphrased from Wikipedia, are geological phenomena in which water-laden masses of soil and fragmented rock rush down mountainsides, funnel into stream channels, entrain objects in their paths, and form thick, muddy deposits on valley floors. Flows can carry material ranging in size from clay to boulders, and may contain a large amount of woody debris such as logs and tree stumps. Flows can be triggered by intense rainfall, glacial melt, and dam break.

Debris flows have highly variable properties. By definition, debris flows have sediment concentrations above 60% by volume (80 weight %) and behave in a plastic (Bingham fluid) manner (Pierson, 2005a). Hyperconcentrated flows occur when sediment concentrations are approximately 20-60% by volume (40-80 weight %) and behave in a manner that is intermediate between debris flows (Bingham fluid) and Newtonian stream flows (Pierson and Costa, 1987 and Pierson, 2005b). However, differentiating between debris and hyperconcentrated flows ultimately depends on flow behaviour, rather than absolute sediment concentration (Pierson and Costa, 1987; Davies et al., 1992 and Takahashi, 2007).

Debris flows are accelerated downhill by gravity and tend to follow steep mountain channels that debouche onto alluvial fans or floodplains and deposit their material (Wikipedia) as flow rates decrease. Conceptually a single event could exhibit the properties of a debris flow, a hyperconcentrated flow and a debris flood (5-10% sediment by volume- Pierson 2005) as it reaches an alluvial fan and/or through dilution as the flow ingests water from the stream channels, especially where large tributaries (in flood) are encountered.

Debris flows transport sediment as a massive, unsorted network of clasts, which can allow boulders to be suspended in a matrix of finer sediment and carried further than would be possible by water flow alone (Pierson and Costa, 1987). Hyperconcentrated flows, like debris flows, are also capable of transporting boulders as well as fine material, although, in contrast to debris flows, boulders are generally transported as bedload (Pierson, 2005b) and sediment is commonly deposited from suspension in the same manner as stream flows (Pierson and Costa, 1987).

While media reports often use the term mudflow to describe debris flows, we emphasise that they are differentiated from true mudflows by their coarser and more poorly sorted sediment load (Rickenmann, 1999).

The speed of debris flows can vary from 5 km/h, to over 80 km/h, and volumes of material delivered by single events range from less than 100 $m^3$to more than 100,000 m^3 (e.g. Rickenmann, 1999).

Factors considered important in debris flow initiation include slope angle, available loose sediment (including deeply weathered bedrock), and degree of land disturbance by activities such as deforestation for agriculture or forest harvesting. Debris flows are typically more frequent following forest and brush fires, as experience in southern California clearly demonstrates (Cannon and Gartner, 2005), and some may be generated by an initial landslide such as the 1872 Glenorchy Debris Flow event (Stevenson et al., 2016). Debris flows are extremely destructive to life and property, and claim thousands of lives every year (e.g. Dowling and Santi, 2014). They are a particular problem in steep mountainous areas subjected to intense rainstorms, and have received particular attention from researchers around the world with several examples cited below.

While debris flows are relatively rare in Australia, including Tasmania, compared to other hazards such as bush fire and flooding, there is sufficient geological and historical evidence to indicate that they are an important geomorphic process operating within the landscape, both in former cold climate and contemporary warm climate conditions (e.g. Wasson, 1977a, 1977b; Moon et al., 1992; Rutherfurd et al., 1994; Mazengarb, 2005 and Stevenson et al., 2016).

Tasmanian Government

Mineral Resources Tasmania

Department of State Growth
www.mrt.tas.gov.au

kunanyi/Mount Wellington debris flow susceptibility and hazard assessment

by C. Mazengarb[1], T. Rigby[2] and M. Stevenson[1]
[1]*Geological Survey Branch - Mineral Resources Tasmania*
[2] *Rienco Consulting - 5 Pelham St, Sorell, TAS 7172*

CONTENTS

CONTENTS cont...

FIGURES

FIGURES cont...

TABLES

1.0 INTRODUCTION

The imposing mountain overlooking Hobart is capped by a layer of dolerite that forms an extensive plateau surface on its summit surrounded by an escarpment. The geology, topography and climate collectively make these steep slopes prone to landslides, rock falls and debris flows. A number of debris flow events are known to have occurred around kunanyi / Mount Wellington since European settlement (including in May 2018), but by far the biggest was the 1872 Glenorchy Debris Flow, originating on the slopes of Mt Arthur and affecting areas along Humphreys Rivulet down to the Derwent shoreline, a distance of around 9.2 km. The historical evidence for this event, the Glenorchy Debris Flow, was comprehensively reviewed in a report by Mineral Resources Tasmania (MRT) (Stevenson, et al., 2016), which provided an understanding of the behaviour of this debris flow and the conditions that prevailed at that time, including the nature of the triggering rainfall event.

Debris flows, such as the 1872 event pose a significant threat to communities situated in their potential runout zones. In order to identify these areas, MRT produced the first debris flow susceptibility maps for Hobart and Glenorchy in 2004 (Mazengarb, 2004a and 2004b) using a methodology described in Mazengarb (2005). This method consisted of employing GIS-based tools for identifying potential debris-flow source areas coupled with a simplistic runout model. The results of this exercise identified a number of urban areas within susceptible zones but the method could not define the likelihood and potential severity of these events.

In response to the release of the 2004 mapping, a validation study was commissioned by Hobart Water (now part of TasWater) using the services of specialist landslide consultants with the assistance of MRT. The review (Fell and Moon, 2007) considered the MRT work was done to a high standard but noted that source areas were underestimated and runout areas overestimated. They recommended further work to be undertaken to improve the calibration of the regional debris flow database with the source area characteristics.

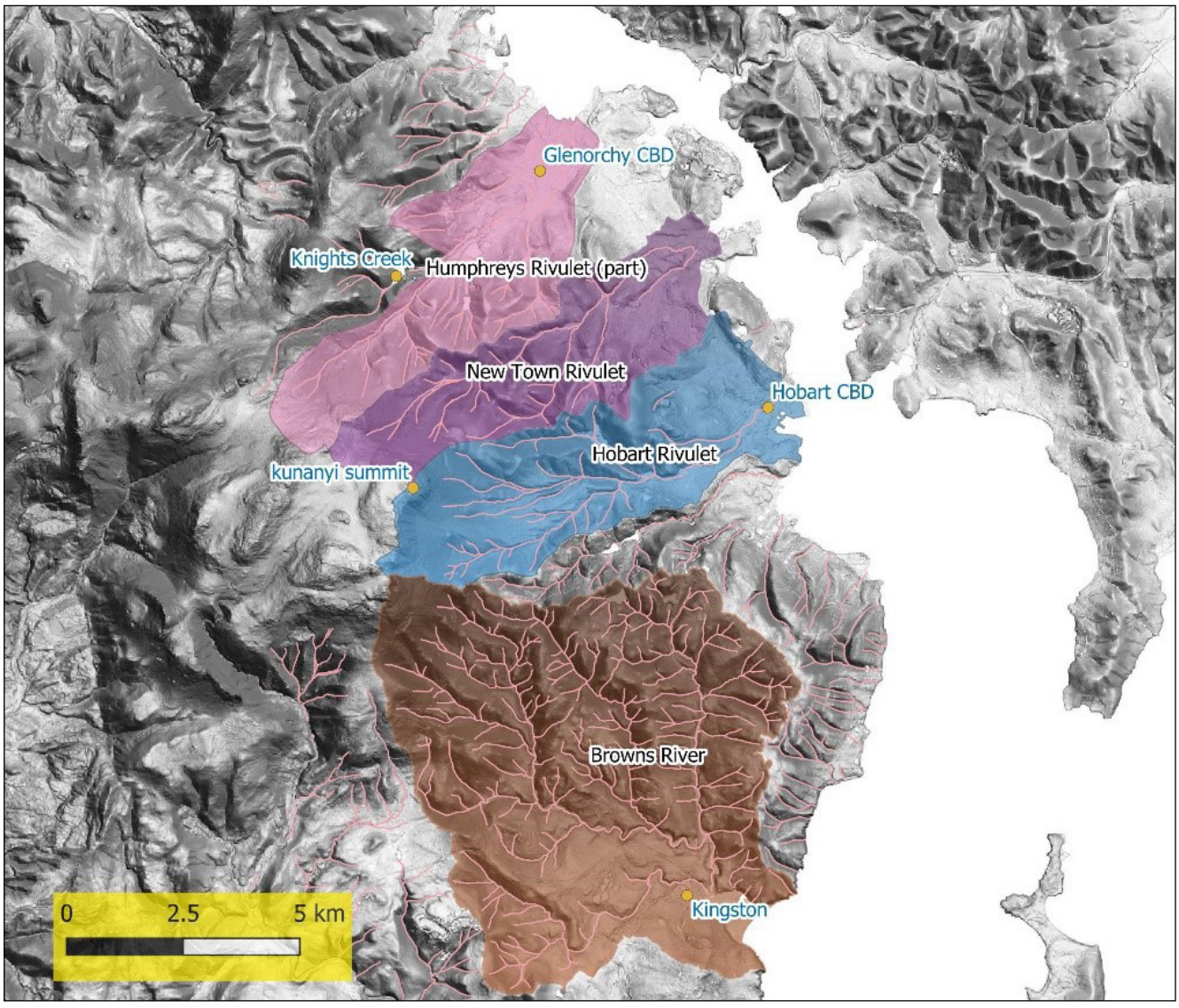

Figure 1. Study area and catchments under consideration.

One of their key conclusions was that the runout distance of the 1872 Glenorchy event was uncharacteristically long for a debris flow and hypothesised that it involved a temporary debris dam that subsequently breached. The existence of a dam was originally proposed soon after the historical event as a possible explanation of the scale and speed of it (as compiled in Stevenson et al., 2016) and at a time when debris flow processes were poorly understood or unknown by the mainly British settlers in Hobart. Based on an analysis of the MRT landslide inventory data, Fell and Moon (2007) produced a probabilistic estimate of future debris flows events occurring in the major stream channels with indicative risk analysis. While we substantially agree with much of their work, later historical analysis of the 1872 event strongly suggests that the event did not involve a debris dam, as the estimated average flow velocity of 55km/hr was well within the range of observed debris flow velocities (Stevenson, et al., 2016).

Since the release of the MRT debris flow maps and the 2007 review, the tools for modelling debris flows have improved and new datasets, such as regional orthophoto imagery and high resolution digital elevation models (DEM) derived from LiDAR (Light Detection and Ranging imagery), have become available. Thus further study and refinement of collected evidence (Stevenson, et al., 2016) allows us to re-examine the previous findings to test their validity as a normal component (monitor and review) of a risk analysis process. In addition, the release of a key guiding document for landslide zoning by the Australian Geomechanics Society (AGS, 2007a and 2007b) provides the architecture for a second generation of debris flow susceptibility maps.

This report documents the evidence and methods used to create this second generation of debris flow maps in the Hobart area.

Please note that all place names referred to in this document can either be found on the map in Appendix 1 or on the Wellington Park map (Anon., 2016).

2.0 METHODOLOGY

We have attempted to follow best practice examples based on published literature and collective experience to produce hazard assessments for the major rivulets draining kunanyi / Mount Wellington ('the mountain') in order to assist the planning and emergency management functions of government.

The approach taken has been to:

1. Review and refine our qualitative understanding of geological and geomorphic processes on the mountain through data collection involving desktop mapping and field validation;
2. Collect and analyse information on past debris flows occurring both within the study area and over a larger area of southwest Tasmania with similar geological and geomorphic characteristics to the mountain, in order to determine statistical properties of these flows;
3. Compare characteristics of the recorded events with those recorded in the international literature as a means of gaining confidence in the data and interpretations;
4. Determine areas of regional and local debris flow susceptibility and, using statistics above, calculate quantitative geomorphic process rates (volume-likelihood relationships) for these areas;
5. Identify appropriate software for modelling the runout of debris flows, using historic records as a means of calibrating the parameters, and then undertake predictive runout modelling for each of the principal catchments in the study area (Figure 1).

3.0 GEOMORPHIC AND GEOLOGICAL MAPPING

Our geological and geomorphic understanding of the study area was reviewed and updated to improve the current understanding of the factors responsible for the occurrence of debris flows. A detailed map has been compiled (Appendix 1) that portrays most of the information collected in the study.

In 2011, a consortium of local and state government agencies initiated by MRT commissioned a commercial provider to obtain LiDAR and photogrammetric imagery of the study area, extending from the mountain summit to the Derwent Estuary. The acquisition served many purposes, but for this project it provided a significantly improved base for our mapping, including an elevation model and complimentary stereo imagery and orthophotos. In particular, the LiDAR provided more detailed morphology of the landscape in forested areas and resulting in the discovery of new features and a greatly improved spatial refinement of previously mapped landslide and debris flows.

The supplied data is publicly available from MRT and from the LIST (Land Information System of Tasmania) under the title: Mt Wellington 2011 LiDAR and Ortho-imagery dataset.

3.1 Geological Revision

Adjustments to the existing published geology have been necessary in this study largely because of the improved base map, but also because the new imagery provides a much clearer expression of the ground surface morphology, especially where covered by forest. Where geological units with contrasting material properties occur together, these boundaries have been

adjusted to follow the morphological expression of this boundary on the LiDAR based DTM with improved confidence. In addition, new observations in the course of field investigations necessitated further adjustment of geological boundaries.

However, despite these improvements, questions remain regarding the boundaries buried under surficial units.

A synthesis of the revised geological and geomorphic mapping is presented in Appendix 1, and a description of the units follows.

3.2 Geological Units

The mapping approach has been to simplify the bedrock units (derived from maps of the Digital Geological Atlas 1:25 000 Geological Map Series: Collinsvale, Longley and Hobart sheets) and move the surficial units into a separate, geomorphological themed layer (Appendix 1).

3.3 Bedrock Units

- Upper and Lower Parmeener Supergroup approximately corresponding to Permian and Triassic ages respectively;
- Tasmanian Dolerite Formation of Jurassic age;
- Mt Wellington basalt (informal) of Cenozoic age. Because this unit is limited to one small area near the summit of the mountain it need not be discussed further.

3.3.1 Parmeener Supergroup

The Parmeener Supergroup is situated on slopes below the Jurassic dolerite, with the most recent and detailed mapping depicted in the 1:25 000 Geological Map Series sheets. Previously, Leaman (1976) published a map and explanatory notes at 1:50 000 scale but neither this, nor the more recent maps and associated reports, discussed the soils formed on these geological units or their susceptibility to landslide failure. Hofto et al. (1991) provides engineering-geology descriptions of the unit over the greater Hobart area, such as its weathering state and physical properties of soils that are summarised herein.

The supergroup is divided into lower and upper units. The Lower Parmeener broadly consists of marine and non-marine sedimentary sequences of fine sandstone, coarse siltstone and fossiliferous mudstone, with occasional thin conglomerate and limestone beds. The upper Triassic unit contains well-sorted quartz sandstone, interbedded mudstone and shale, with feldspathic sandstones in the higher in the sequence.

Exposures of the Supergroup on the upper part of the mountain are limited as much of the area is blanketed by surficial colluvial deposits. However, an exception is the Knocklofty Formation sandstone (Triassic) that forms locally impressive bluffs such as at The Springs, Sphinx Rock and Crocodile Rock (Figure 2).

Figure 2. Upper Parmeener sandstone outcrop with soft sediment fold, Crocodile Rock - Hunters Track.

Hofto et al. (1991), concluded that weathering of Permian rocks is usually uniform, shallow and locally units may weather deeply to clay (CH) or gravelly clay (GC). Triassic sediments tend to weather irregularly as a result of variations in rock types; sandstone units exhibit a thick and gradational weathering profile, largely of clayey sand (SC), while the mudstones are particularly susceptible to weathering, often forming thick clay horizons. Weathering depth may vary, with clay ranging up to several metres in depth.

Hofto et al. (1991) also provides XRD analyses of clay minerals formed in the soils (Figure 3). According to these results, montmorillinite and kaolinite are the major clay minerals identified. We note that the semiquantified results presented in Figures 3 and 7 are indicative in terms of the relative abundance of these minerals, as some of the records clearly do not add up to 100%. There is also some question regarding the identification of these minerals given that the analyses were undertaken about 3 decades ago. Specifically, montmorillinite may be better classed as smectite whereas it is possible that kaolinite may in fact contain an unknown component of halloysite. Regardless of this uncertainty, the properties of these particular clay types in soil profiles have important relevance to slope instability.

3.3.2 Tasmanian Dolerite

Jurassic Dolerite caps the upper 300 m of kunanyi/ Mount Wellington and is well exposed on parts of the escarpment (e.g. Organ Pipes) and on the plateau landscape capping the mountain. However, the basal intrusive contact is largely concealed under slope deposits. While there is a major break-in-slope forming the base of the dolerite escarpment, this does not coincide with the base of the dolerite, the latter being typically lower by many tens of metres. This is a somewhat puzzling observation given the contrasting material properties with the underlying Parmeener rocks. This relationship is not fully understood.

Surface exposures of dolerite consist of vertical columns of extremely high strength (EH) slightly weathered (SW) dolerite rock (Figures 4 and 5). Columns range from 1 and 3 m in diameter. While fresh dolerite outcrop dominates the landscape there are instances where significant weathering profiles 3-4 m deep (and inferred to be deeper), have developed, such as at the source area of the 1872 Glenorchy Debris Flow (Figure 6). Such areas on steep slopes must be regarded as potentially unstable but as exposures are very limited it is difficult to map these areas with confidence. For instance, in a walk-over of the 1872 Glenorchy Debris Flow scarp, it was noted that the weathering profile was highly irregular and without any obvious predictability over short distances.

Hofto et al. (1991) recorded the dominant clay minerals formed through chemical weathering of dolerite being montmorillinite and kaolinite (Figure 7) and soils with these constituents can become unstable on relatively low slope angles. However, as with the analyses of Parmeener Supergroup sediments, other clay minerals such as halloysite and smectite, may have gone unrecognised.

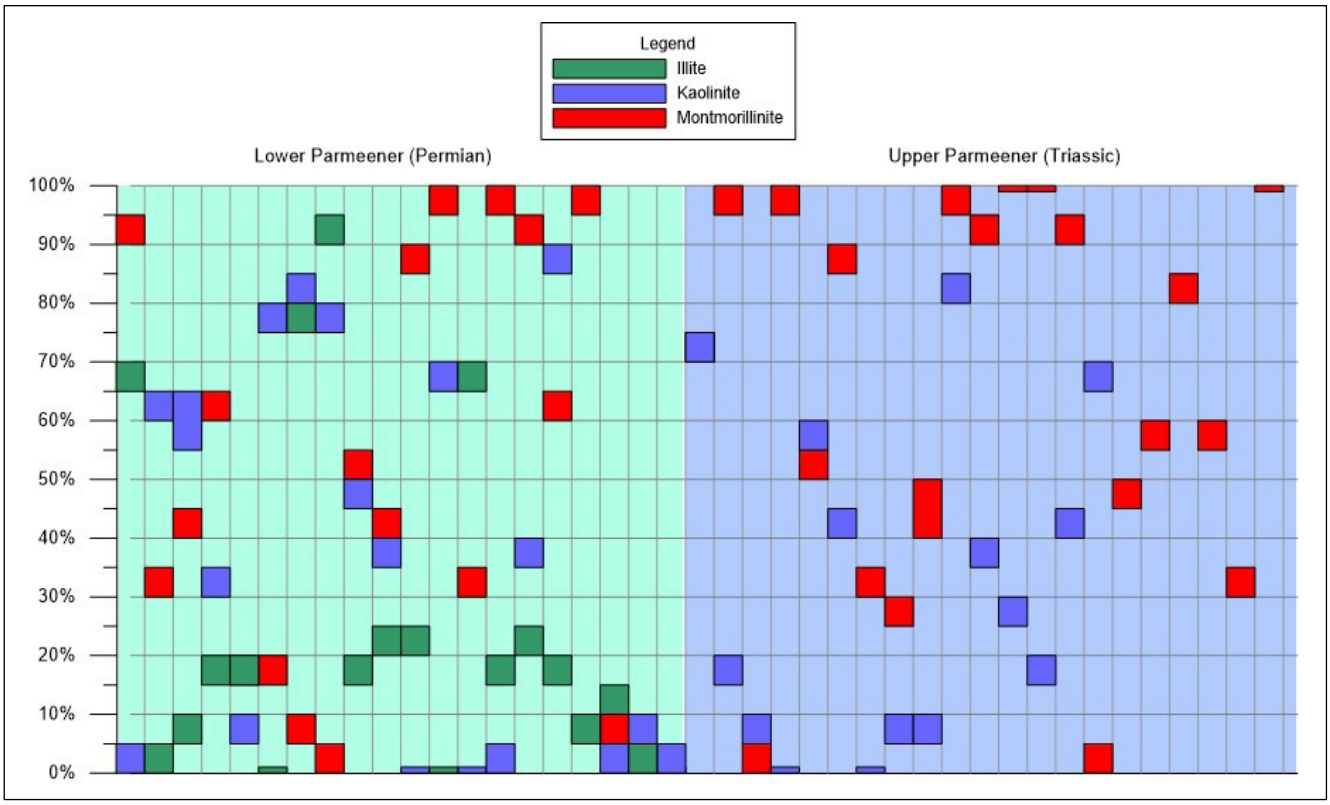

Figure 3. Semiquantified XRD analyses of clay minerals formed from weathering of Parmeener Supergroup summarised from Hofto et al 1991. Each column shows the results for an individual sample.

Figure 4. Upstanding dolerite columns at the top of the escarpment.

Figure 5. Dolerite columns, with irregular forms, the result of long term weathering processes.

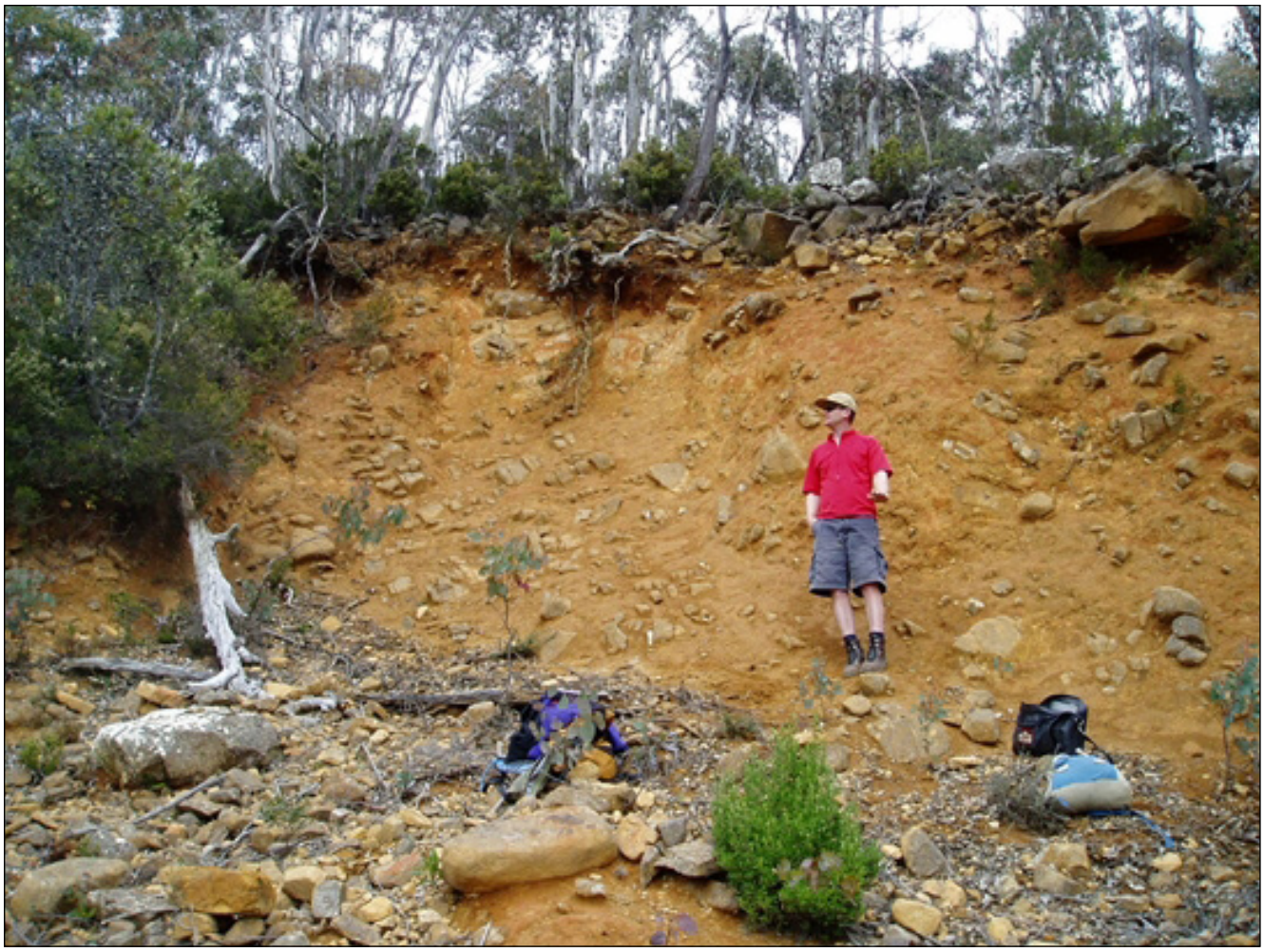

Figure 6. Extremely weathered to highly weathered dolerite (bedrock structure barely recognisable) overlain by solifluction boulders at top of outcrop.

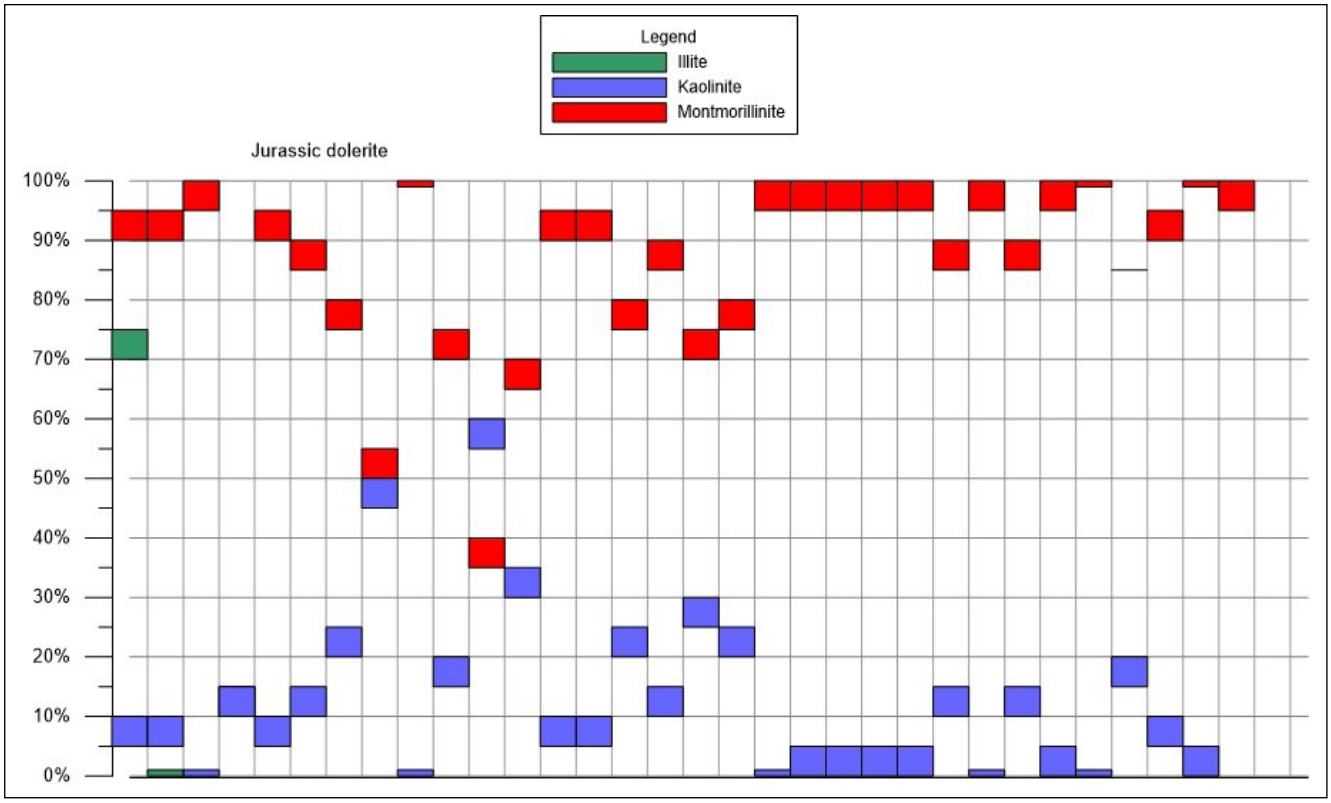

Figure 7. Clay minerals identified by semi-quantitative XRD in dolerite derived soils in the greater Hobart area by Hofto et al. 1991. Each column shows the results for an individual sample.

3.4 Surficial deposits and related geomorphic features

This section describes the surficial deposits encountered on kunanyi / Mt. Wellington's slopes along with other morphological features and discusses their likely origin.

Surficial deposits are widespread in the area but are highly variable in nature and thickness. The geological mapping approach adopted separates surficial from bedrock units to create a separate thematic layer so that the former can be more fully delineated without compromising the known or inferred extent of bedrock units.

While newly acquired remote sensing imagery has allowed us to better map the extent of these deposits in detail, they are in places difficult to map, let alone separate into different units. Some deposits are obvious in unvegetated areas, but were difficult to recognise where they extended into surrounding forests. While a field mapping exercise was undertaken, the challenging terrain and limited exposure made it difficult to substantially map the full extent of these units on the ground. Furthermore, the output scale of the attached maps meant that not all deposits could be usefully displayed.

An inspection of new exposures in New Town Rivulet after the May 2018 rainstorm provided a window into the complexity of these deposits both vertically and laterally, demonstrating the difficulty in reliably tracing them across the landscape with available methods (Figure 8). The contrasts in textures, clast size, sorting and matrix composition suggests different mechanisms of emplacement have operated over time, with the middle unit interpreted as a block field deposit that is possibly an extension of that mapped further uphill.

The following informal units of Pleistocene age have been recognised:

- Topple deposits;
- Block deposits of probable periglacial origin including block streams, block slopes, block fields and apparent mass movements;
- Colluvial deposits (undifferentiated) with or without matrix;
- Alluvial deposits (not discussed but forming the outwash deposits of mountain slope processes).

3.4.1 Topple deposits

These features occur at high altitudes adjacent to, and downhill from, in-situ dolerite escarpments. The deposits are distinctive in consisting of bands of elongate forward tilted columns, ranging from semi-detached to completely detached. The escarpments from which these deposits occur may be as little as a few metres in height but range up to tens of metres elsewhere. The deposits have formed through a toppling process, whereby individual or interlocked groups of columns have forward tilted away from the bedrock and eventually detached. It is not uncommon to find in places a complete progression of columns in a downhill direction, from in-situ upright form, increasingly forward tilted (but not detached) and completely tilted and detached (Figures 9 and 10).

Stevenson (1980) provides examples of varying mechanisms of toppling including the Lost World topple that is an extreme (large) version of this process and which is described separately below.

Figure 8. Fresh exposures of surficial deposits in New Town Rivulet formed during the May 2018 flood. In-situ doleite is exposed at right where the (1 m long) blue walking staff rests. At least 3 surficial units are evident in this exposure.

Figure 9. Forward tilted columns on edge of escarpment.

Figure 10. Topple deposits (right) below in situ columns (left and foreground).

3.4.2 Block field deposits

These features occur both on the subdued landscapes above the dolerite escarpment on slopes as low as 3 degrees and on the upper and mid slope positions (Figures 11 to 13). They consist of randomly oriented, well sorted and sub angular boulders of dolerite of up to 2 m dimensions with varying proportions of fine matrix. They are best observed above the tree line and in distinctive non-forested areas below. Our field observations and LiDAR imagery indicates that they also occur in forested areas but are more difficult to delineate.

One such example at the head of New Town Rivulet demonstrates a typical geometry whereby the block field on the shallow sloping plateau narrows in a downhill direction as the landscape steepens and enters into the rivulet.

On some steeper slopes we have observed areas where undulations on the surface occur in arcuate form parallel to the contour and in straighter forms parallel to the slope direction. These areas have characteristics of mass movement as they can include an arcuate, steeper area at the top of the feature resembling a headscarp. In other instances we observe lobate forms at the downhill limit of the features.

The block-fields have been interpreted as the products of solifluction (or periglacial geomorphology) processes by Davies (1958). Barrows et al. (2004) has discussed the ages of these deposits, suggesting that there are at least two phases of generation with exposure dates of three columns on the mountain top ranging between ~90kyr and ~500kyr.

Periglacial material by definition is driven by the forces of gravity and freeze-thaw weathering, with various amounts of interstitial ice and snow separating the angular dolerite clasts. Currently only the highest parts of the mountain have such processes operating (where it is cold enough) but this would have extended much lower during previous cooler climate periods in the Pleistocene. Our mapping shows that the majority of deposits occur above 750 m elevation and the lowest around 600 m, an observation consistent with a regional assessment by Colhoun (2002). Some of the areas with apparent mass movement morphology may be related to nivation hollows (e.g. near Plains Rivulet) where substantial thicknesses of snow and ice possibly accumulated along with intercalated rock material in past cooler climates. With subsequent warming the ice has melted creating a deflated morphology.

These surficial materials range from containing fresh rock debris without any interstitial matrix, to chemically weathered material surrounded by a fine clay matrix. Where these deposits are devoid of a substantial fine matrix, they are generally on slopes well below their angle of repose. Alternatively, where the deposits are significantly weathered, the material has been significantly weakened and may be close to- or exceeding their angle of repose, making them potentially susceptible to slope failure.

In many instances the thickness of these deposits is uncertain and the geological units they overlie may be poorly understood. However, we consider overall that they are usually only a few metres thick on most slopes, except in local hollows such as the Devils Gulch where conceivably they may range up to 10 m. Where they overlie material of low soil strength then they are potentially susceptible to slope failure.

As we have previously discussed there is difficulty in mapping these features in the landscape including delineating where more weathered material might exist. Other than limited field observations along track cuttings, landslide scarps or streams, a significant clue is the presence of gully erosion in the heads of a few streams that can be observed in the LiDAR imagery and confirmed by field inspection.

3.4.3 Colluvium

By far the most extensive of the surficial deposits are the colluvial deposits. The term is used collectively to describe a variety of slope deposits that may include any of the surficial units described previously. In general the colluvium contains a variety of poorly sorted material ranging from metre size blocks of bedrock, to a clay matrix. A particular mechanism of formation is not implied; some could be periglacial in origin, some creep and some debris flow deposits. The thickness of these units is highly variable and may range up to a few metres at most.

These deposits extend down to low altitudes, particularly in the Hobart catchment, encroaching on fringing suburbs at South Hobart. We do not know how old these deposits are, whether they formed by fast moving or slow mechanisms, or if they formed in an absence of forest cover. If they are the product of fast moving debris flow deposits this raises several questions as to the susceptibility of these areas to modern events that we are not able to confidently answer.

3.4.4 Alluvium

We have shown the distribution of alluvial deposits on our map, mainly taken from the MRT 1:25 000 geological map series (cited in full previously) and in places modified to match the new basemap. These deposits are described in the legends of the constituent maps and occur mainly on the lower slopes of the mountain. They are interpreted to represent the fluvial outwash of surficial material derived from the upper slopes of the mountain.

Figure 11. Uphill extent of block field development near South Wellington (the 'Ploughed Fields').

Figure 12. Block field development on slope below previous figure (‘Ploughed Fields’).

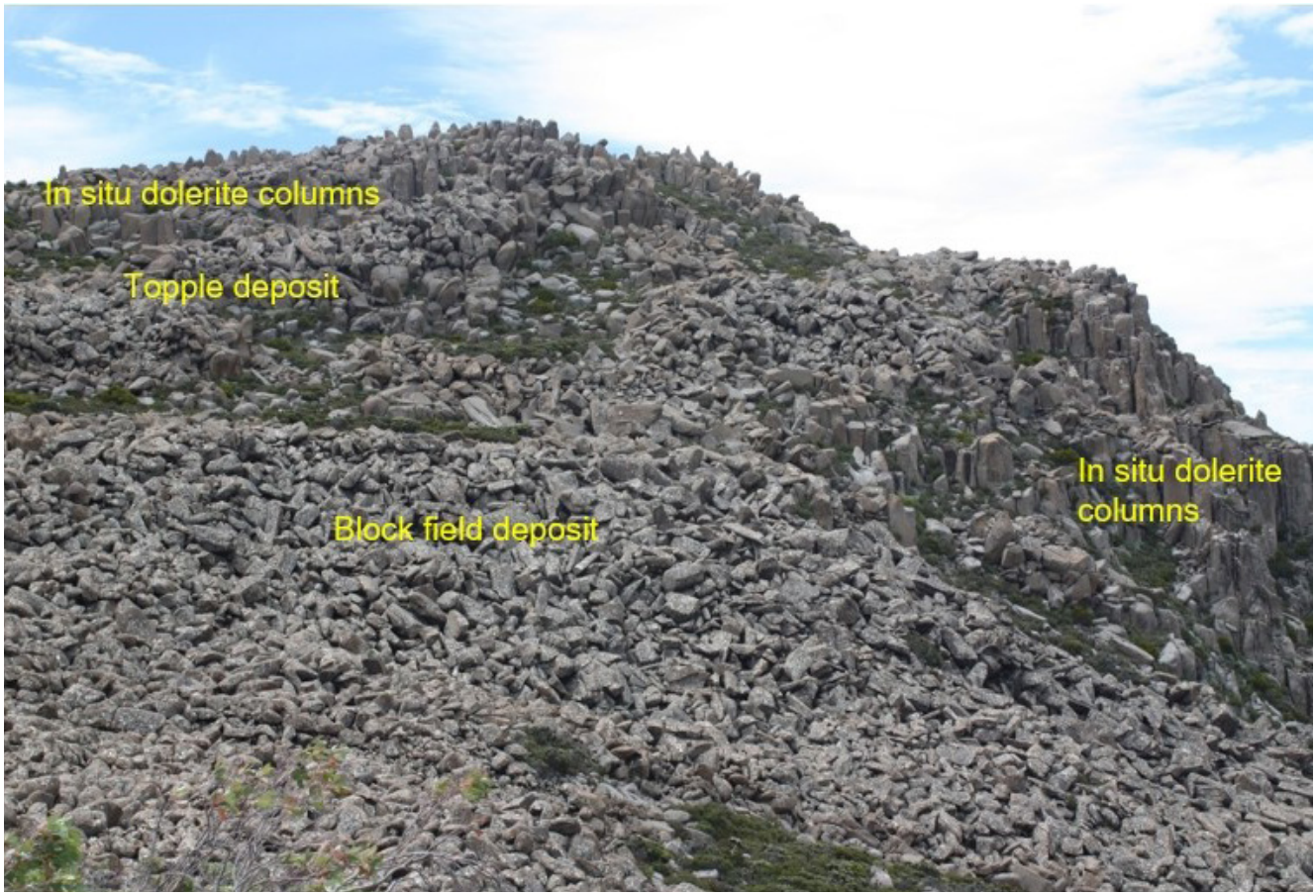

Figure 13. Relationships between in situ dolerite bedrock, topple deposits and block fields near top of the Ploughed Fields.

3.5 Other Features

We show other landscape features on the map (Appendix 1) and these features are also stored in the MRT Landslide Database (available online):

- Large block topples such as the Lost World Landslide. These possibly formed through periglacial processes and are widespread on the upper part of the mountain;
- The source area of the 1872 Glenorchy Debris Flow where failure of colluvium and weathered bedrock has occurred;
- Gully erosion in the heads of significant tributaries. In this instance, we consider that the process is associated with the initiation of debris flows, based on the experience of the 1960 and 2018 rainstorms, both of which triggered debris flows in branches of New Town Rivulet;
- Debris flows scars;
- Breaks in slope and textures that allow us to improve the knowledge of material distribution (both bedrock and surficial geology);
    - ◊ Cliffs lines such as those above the Organ Pipes where rock fall sources are concentrated;
- Tors on the plateau.

3.6 Geomorphological Synthesis

Some aspects of geomorphology have already been discussed and the following will focus on upland terrain where the most energetic and probably damaging debris flows originate. A simplified cartoon of the slope processes is to be found in Figure 14.

3.7 Long Term (Cenozoic) Retreat of the kunanyi / Mount Wellington Escarpment

The dolerite capped escarpment probably formed in Paleogene times (Paleocene to Eocene) associated with the creation of the Lower Derwent Graben (Forsyth, et al., 2014). Once formed, the escarpment has retreated through erosional processes over geological time with accompanying transportation of bedrock-derived material into the Derwent Graben and surrounds.

1:25 000 scale geological mapping by MRT indicates the western side of the approximately north-south trending graben is a complex fault system that lies about 2 km east of the present escarpment. The amount of vertical offset along this fault zone is difficult to precisely constrain but may range up to 1 000 m. If an absolute age of between 55 and 60 million years was adopted for initiation of the fault system, and formation of the escarpment, it would indicate a long term retreat rate of approximately 35 m/Myr. While it is certain that this rate has varied during contrasting climatic regimes,

this type of estimate serves to provide a constraint on geomorphic process rates on kunanyi / Mount Wellington and the determination of design events for debris flow and rock fall.

3.8 Cold Climate (Pleistocene) Landscape Evolution of the kunanyi / Mount Wellington Escarpment

During the last 2.5 million years there have been a number of global climatic cycles, referred to as glacial and interglacial periods. As discussed previously, the kunanyi / Mount Wellington plateau has deposits resting on it ranging at least as far back as half a million years (Barrows, et al., 2004) indicating that material in the near surface of the plateau today has been affected by at least 3 glacial episodes. In the upper parts of the mountain, the cold climate conditions were such that periglacial processes operated. These were sufficient to trigger mechanical weathering of in-situ bedrock in the near surface, with column toppling and flaking of surfaces being particularly important. This process liberated material that has subsequently been transported downhill to form the block-fields, rock fall deposits, debris flow deposits (e.g. Wasson, 1977a and Wasson, 1977b). The migration of material downhill has resulted in formerly incised stream channels being choked with sediment in their upper parts. This material has the potential to be remobilised by the processes discussed below.

3.9 Warm Climate (Pleistocene and particularly Holocene) Landscape Evolution of the kunanyi / Mount Wellington Escarpment

Holocene and previous interglacial climates were not only warmer but usually wetter than modern condtions. In these conditions the relative importance of chemical over mechanical weathering is presumed to be greater due to reduced freezing and thawing but also to an increase of free water at warmer temperatures flowing though the rock mass and surficial material. Chemical alteration and breakdown of this primarily doleritic material along in situ bedrock defects and the perimeters of displaced material produces weakened material and low-strength clay minerals, some of which have subsequently mobilised to infill cracks, migrate downhill to be included in the matrix of the surficial deposits or washed down to the sea.

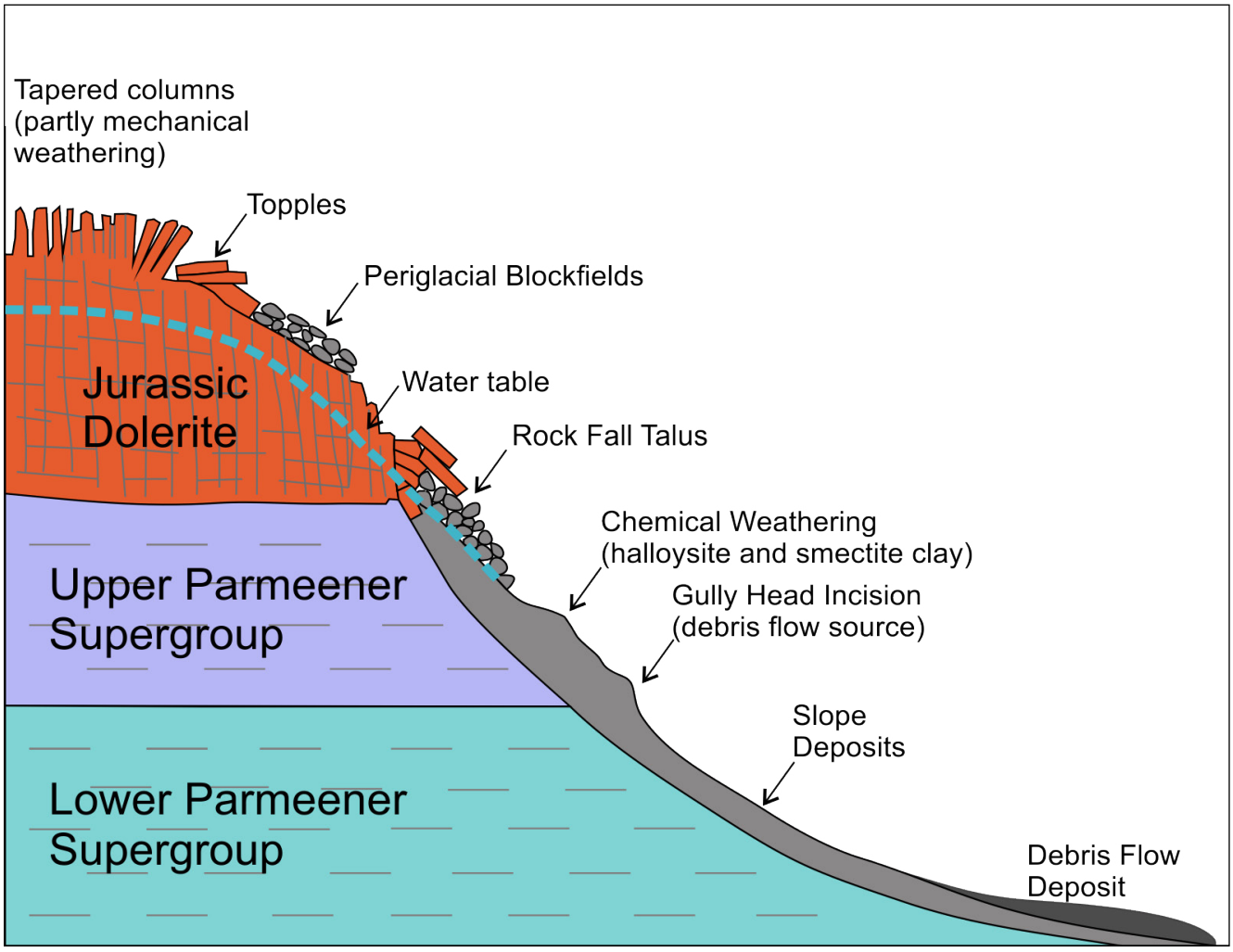

Figure 14. Schematic simplified slope process model. Not to scale with significant vertical exaggeration.

Where chemical weathering is advanced, this has led to reduced strength of the rock mass and surficial material, making it vulnerable to slope failure.

The transition from cold climate to warmer climate conditions can conceptually generate an accelerated phase of erosion on hillslopes as subsurface and surficial flow rates increase. During this transition, the lowered tree line has yet to recover and thus provides less protection to erosion and mass movement on the higher slopes. Furthermore, the protection offered by forests to resist debris avalanches coming from higher up the slope will also be reduced, and this may explain the large lobe of colluvium extending down to South Hobart described previously.

However, there is another mechanism that appears to dominate during recent European recorded history, and possibly over much of the Holocene, and this is occurring in the stream channels as gully erosion. The likely increase of water flowing down channels associated with rainstorms is triggering headward erosion of streams, some of which become debris flows, in the segments that were previously choked with sediment. This process results in the stream channel progressively returning to its previous base level and cutting back to bedrock (see discussion below). For several streams on the mountain there is some distance to go before the source of readily-erodible material infilling the channels is exhausted.

3.10 Concluding Remarks

Our review of the geology and geomorphology of kunanyi / Mount Wellington identifies materials and processes that predispose it to a range of slope processes including debris flow. The following sections of the report document evidence for debris flow phenomena in southest Tasmania and use the collated metrics to predict process rates, volumes and runout behaviours.

4.0 LANDSLIDE MAPPING, ANALYSIS AND PREDICTIONS

This section addresses the methodology for collection of data on debris flows, what was recorded, how it was analysed and how it is used to make predictions of future events.

4.1 Landslide Inventory

In 2004 MRT undertook a reconnaissance study to identify debris flows on dolerite-capped mountains in eastern Tasmania using aerial photographic surveys held by Land Tasmania and Forestry Tasmania as it was previously known. Much of this work was done by our former MRT colleague Dr Clive Calver to whom we are most grateful. The purpose of the work was to provide supporting information to enable debris flow susceptibility maps on kunanyi / Mount Wellington to be produced using parameters based on empirical evidence. Air photos captured between 1945 and 2003 were inspected and over 300 features recognised that were interpreted as either debris flows or debris avalanches.

These features were transferred from the unrectified aerial photos onto 1:25 000 topographic base maps, digitised into GIS format, and entered with attributes into our landslide database. Most of these features have not been inspected in the field because of their remote locations. The dataset includes the following:

- point locations of the source area (GIS layer);
- polygon outline of the entire feature (affected area) (GIS layer);
- travel angle estimation;
- including whether the flow has become channelised;
- width of the source area;
- slope of the source area;
- catchment area upstream (derived subsequently);
- geological setting;
- timing constraints on the formation of each feature based on first appearance on aerial photos or other data sources.

The study has not been previously published in it is entirety but the landslide features are publicly available via MRT's online landslide database and aspects of the results are covered by Mazengarb (2005). Parameters derived from the dataset were used by Fell and Moon (2007) to support their debris flow study, in particular travel angle and volume analysis.

In undertaking the current study we have reviewed this earlier work, given that it is over a decade old, in order to better assess its reliability and currency. We make the following comments:

- In checking the location of points and polygons against more recent and more accurate orthophoto bases (made available by Land Tasmania, DPIPWE) and Google Earth satellite imagery, the location of the features may be as much as 50m away from their true position. We also noticed that the width of the features appeared to be slightly exaggerated in a number of cases. We have subsequently adjusted many of these features where they are obvious on subsequent imagery and updated their morphometric parameters, taking advantage of improved DEMs to estimate elevation, slope and contributing areas.

- A significant population of the landslide features are in native forests where the canopy has been removed exposing earth/rock material that provides high contrast and improved detection. However, with time these areas become increasingly revegetated and degraded hence it becomes difficult to detect, accurately locate and determine their critical morphometric parameters. In particular, the area of depletion (source area) is often poorly constrained because the length is difficult to constrain (on the downhill end) compared to the width. Furthermore, volume estimates are even more difficult to obtain from aerial photos and topographic maps except where good quality LiDAR DEMs are available. There is also difficulty in a number of instances in determining the full extent of the runout zone (and hence the travel angle estimation) as it is not always obvious where the flow terminates, especially once material enters a significant stream channel. In these instances, subsequent or concurrent stream erosion can either destroy the debris flow toe (leading to an underestimation of the travel distance) or carry sediment further downstream (possibly leading to an overestimation of travel distance).
- We followed the advice of Guzzetti (2005, p. 97): '...where smaller landslides sit within larger features they must be separated to obtain the area of each feature; large landslides must be carefully checked to ensure that they are not amalgamations of smaller features or digitisation errors'.

Subsequently, mapping for our project identified additional features on kunanyi / Mount Wellington with the benefit of LiDAR imagery that were added to the landslide inventory. More landslides were also recognised over the wider area as observed in satellite imagery (Google Earth) and subsequent aerial photographic surveys.

In all, 225 debris flow events are recognised within the southeast Tasmania area that have occurred within a time period of around 80 years. A further 149 features are older, all of which, except for the 1872 Glenorchy Debris Flow, are undated.

The definitions and metrics of debris flows stored in our landslide inventory are outlined below (Figure 15; Table 1) and are an adaptation of the IAEG Commission on Landslides (1990) explained in Cruden and Varnes (1996).

Table 1. Defining terms used in Figure 15.

Ref. No. from Cruden & Varnes	Name	Description
2	Width of surface of rupture, Wr	Width of the surface of rupture
4	C-F Length, Lr	True length of surface of rupture (Crown to beginning of Foot). Directly measured or calculated from other parameters
10	C-F Distance, Ld	Distance of surface of rupture on map (Crown to beginning of Foot)
6	Depth of surface of rupture, Dr	Maximum distance from former ground surface to surface of rupture
7	C-T Length, L	True Length from Crown to Toe, (accounting for elevation change).
12	C-T Distance	Crown to toe distance in map view (typically a sinuous line following centreline of channel)
N/A	Travel Angle, alpha	The angle defined by C-T Elevation /C-T Distance
N/A	Angle Original Ground Surface (OGS)	Estimate of the original ground surface slope in the Area of Depletion
N/A	C-T Elevation (deltaE)	Elevation difference between crown and toe

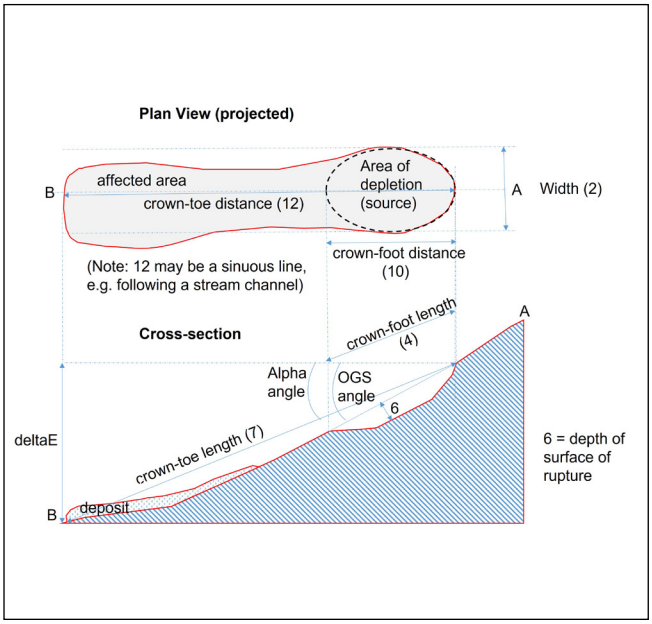

Figure 15. Landslide metrics and definition.

4.2 Volume Calculation

The determination of volume for a given landslide (including debris flows) is a powerful metric used for several purposes in landslide analysis. However, it is not an easy metric to obtain especially from largely remotely sensed data.

Cruden and Varnes (1996) provide an equation for volume estimation assuming a half-ellipsoid approximation (Figure 16) that is widely used by landslide researchers.

Volume = 1/6*Pi*Depth*Width*Length geometry

While landslide width (W) can, in almost all instances, be confidently measured (for fresh landslides), the metrics of Length (Lr) and Depth (Dr) are recorded in order of decreasing reliability. Fortunately the international literature provides approximate methods of estimating volumes where incomplete information is available and those records where 2 or all 3 parameters are known can be used for validation purposes.

Klar et al. (2011) conclude that landslides have a degree of self-similarity, in that the ratio between length and width remains similar regardless of size. From a limited review of similar studies to our own, the ratio of L/W varies from 2 (e.g. Hovius, et al., 1997 and Timilsina et al., 2014) to 3 (Fell and Moon, 2007). With the benefit of our improved inventory a limited number of debris flows have length and width determined. Our analysis reveals that a ratio of ~2.5 provides the best linear fit for our dataset (Figure 17).

Whereas Length and Width ratio may be self-similar, Klar et al. (2011) amongst others conclude that depth deviates significantly from a self-similar relationship and in three dimensions landslides are self-affine. Specifically, as the landslide increases in area, depth does not scale at the same rate.

To address this observation Fell and Moon (2007) proposed the following logarithmic relationship between width and depth (Dr) that reflects a self-affine scaling principle although it is not clear how the calculation was determined:

Depth (Dr) = 0.4 + ln(W)

In our study, with the benefit of more information, we have charted Width vs Depth (Dr) to establish a best fit logarithmic relationship honouring our data (Figure 18).

Depth (Dr) = 5.39894576 * ln(W) – 13.721170606

It is acknowledged that there are only a small number of landslides in our database (n= 10) for which depth has been determined in one way or another. As can be seen the data is not well distributed and the two largest landslides strongly control the shape of the fit. Despite these limitations, it is obvious that there is a significant difference with the Fell and Moon (2007) interpretation.

Based on parameters obtained above and aware of all the underlying assumptions, we have produced volume estimates for our control set of landslides to compare against those used by Fell and Moon (Figure 19). Both indirect methods compared to the half-ellipsoid method show cross overs against the ideal line as volumes increase but in opposite directions. When compared against each other our study has smaller comparative volumes at the lower part of the distribution and larger volumes at the upper part of the range. The impact of this will be assessed in the following magnitude – frequency analysis.

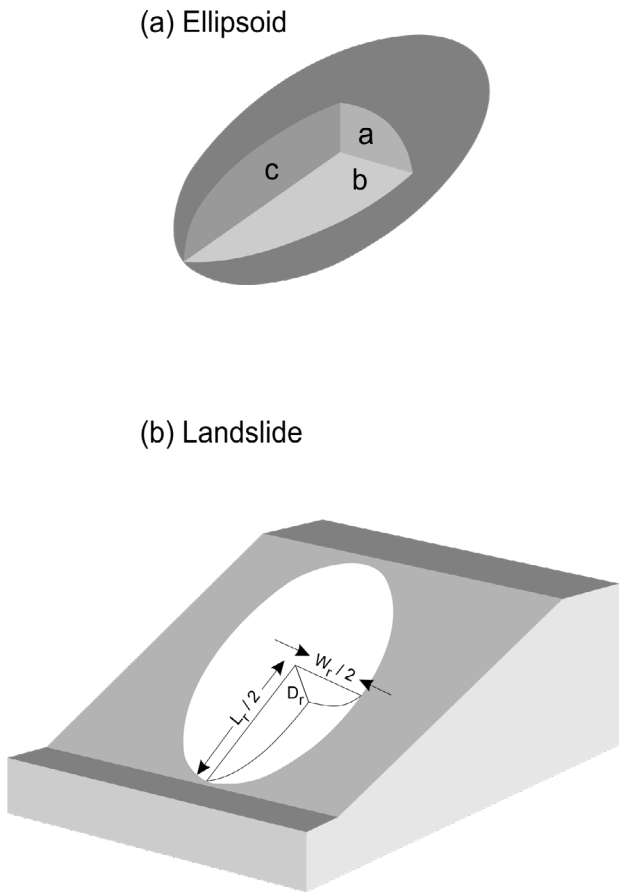

Figure 16. The half ellipsoid landslide volume approximation from Cruden and Varnes (1996, Figure 3.6).

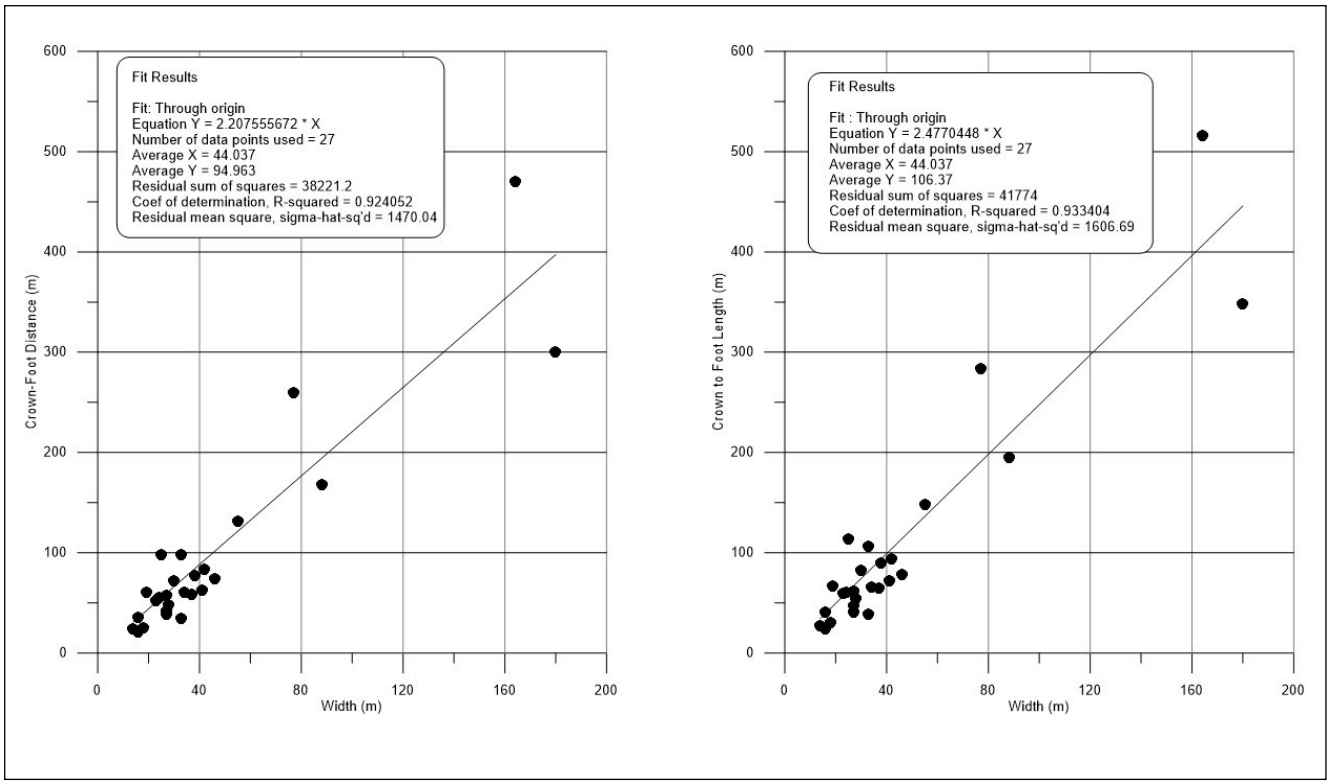

Figure 17. Width-Length relationships for source areas; Crown to Foot Lengths (right) were calculated from Crown to Foot Distances using a local slope correction parameter.

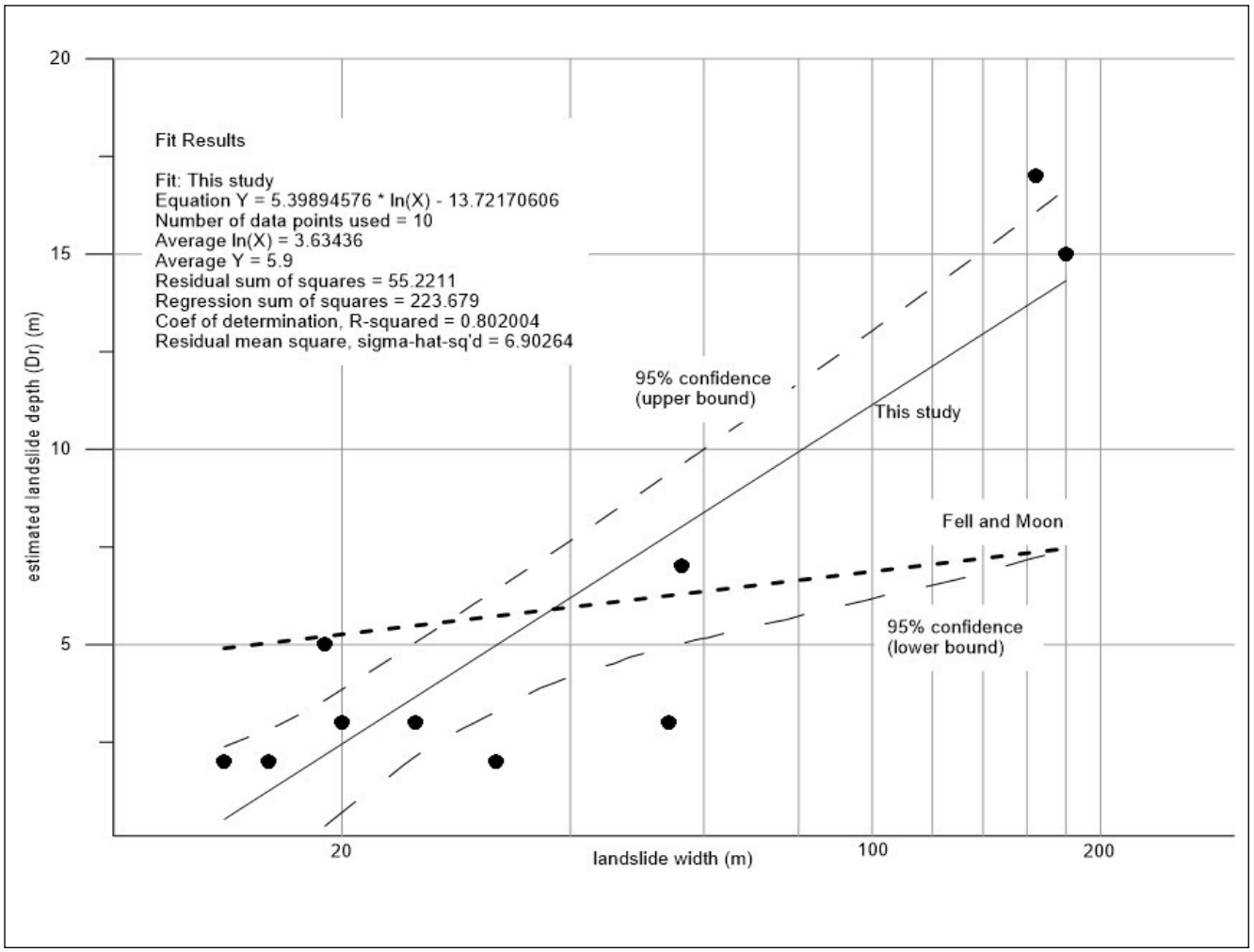

Figure 18. Landslide width - depth relationships using data from this study.

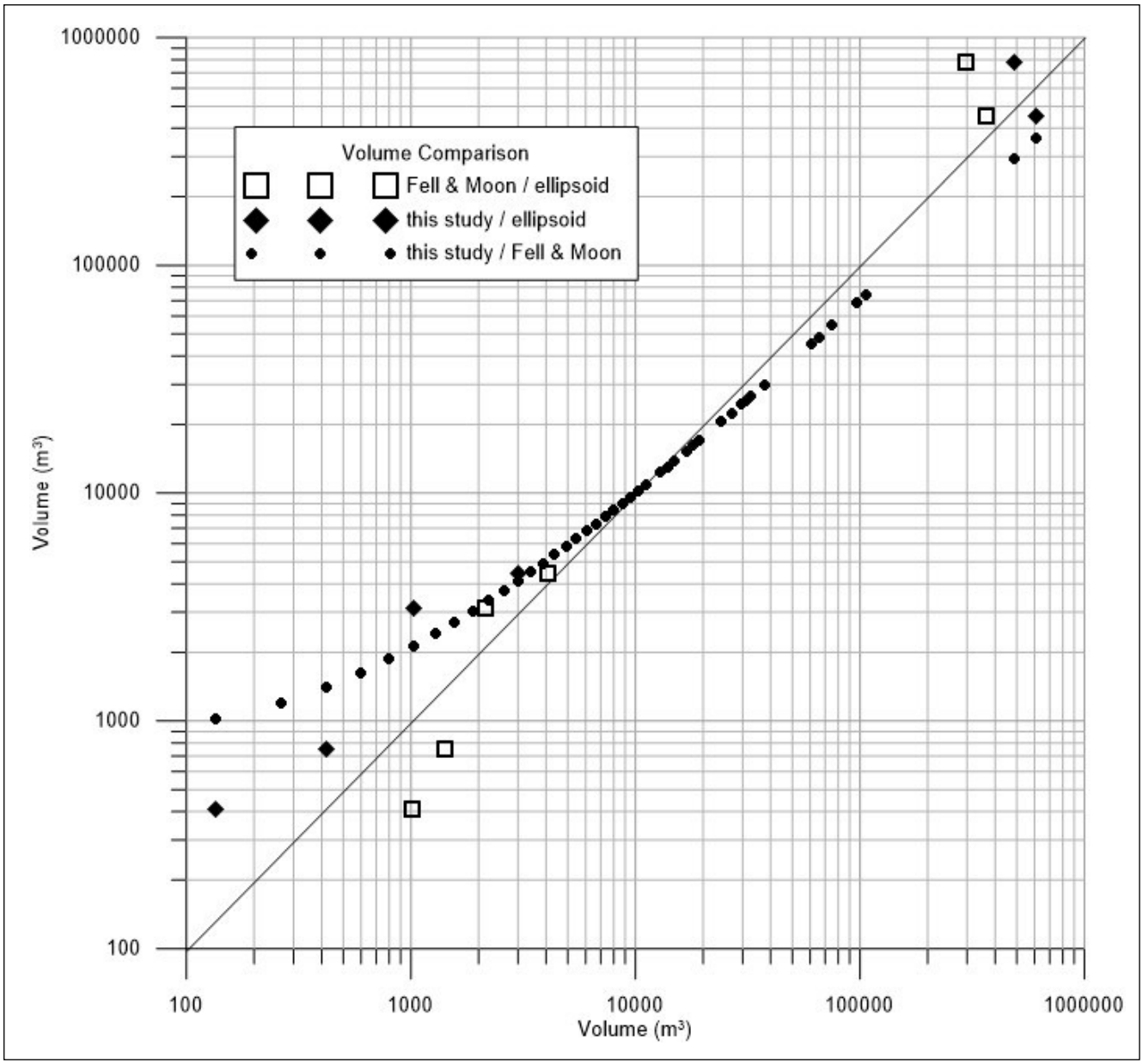

Figure 19. QQ plot comparing methods for estimating debris flow volumes. Ellipsoid method refers to records where all three parameters of the ellipsoid are recorded in the database. The first method in each case is plotted on the X axis.

4.3 Runout and volume relationships

In this section we examine the derived metrics, particularly volume and runout, of our landslide inventory that will constrain the choice of parameters in the ensuing debris flow modelling. We have also undertaken an assessment of respected, peer reviewed papers to determine how well our dataset compares with others in order to provide a level of confidence for our study.

Our empirical dataset of debris flow runout values for Tasmania is presented in terms of a cumulative distribution (Figure 20). This distribution indicates that all but one of our records have travel angles >= 12, the exception being the 1872 Glenorchy Debris Flow. The quartiles identified are very similar to those presented in Mazengarb (2005) and were used as a basis for the deterministic models in the Hobart and Glenorchy debris flow maps (Mazengarb 2004 a,b). The plot also shows that channelised debris flows tend to be more mobile with lower travel angles.

A number of empirical studies conclude that with increasing volume, landslides of various types have greater runout mobility (e.g. Corominas, 1996; Rickenmann, 1999; Hunter and Fell, 2002; Rickenmann, 2005 and Takahashi, 2014). These authors, amongst others, have used a variety of methods to quantify the relationship.

Corominas (1996, his Figure 6) provides possibly the cleanest dataset of those reviewed. The dataset is mainly based on mapping in the Pyrenees of northern Spain, showing only debris flow and debris avalanche events and plotting reach angle (elevation difference/travel length) against volume. He has further categorised his data according to obstacles and topographic constraints of the path, including whether the features are channelised or not. For comparison, we have categorised our data set into obvious channelled and non-channelled groups but not his other categories (Figure 21).

It can be observed that:

- our dataset is broadly very similar to the Spanish dataset;
- our channelized flows are mostly larger by volume than our non-channelised ones;
- the channelled Glenorchy debris flow (assuming it is a single event), with parameters: L = 9100 m, M = 210 000 m^3 and H = 900 m, fits within the range of Corominas' channelised flows.

Rickenmann (1999) provides a synthesis of a range of landslide features (including debris flows) from Europe and North America, along with laboratory measurements plotting runout length against volume times elevation difference. His chart (Figure 22) suggests that the 1872 Glenorchy Debris Flow (as we have interpreted it) falls within the natural range of debris flows. In a later study (Rickenmann, 2005; Figure 23), he shows that the same debris flow falls slightly outside of the 95% confidence bound for the Corominas (1996) dataset, but is still within the range of these types of features.

Similarly, both Hunter and Fell (2002) and Takahashi (2014) provide evidence that the 1872 Glenorchy Debris Flow falls within the natural range of debris flows (Figure 24).

The evidence from these five studies is that the 1872 Glenorchy Debris Flow has a runout – volume relationship, that while rare is not precluded, and the proposition that the 1872 event travelled as a single event for the entire distance from its source to the Derwent Estuary is compatible with the literature reviewed. While we cannot rule out a two stage process involving a debris dam (the Fell and Moon (2007) model), this conclusion, coupled with our historical study (Stevenson et al., 2016), indicates that there is no necessity to invoke a more complex mechanism.

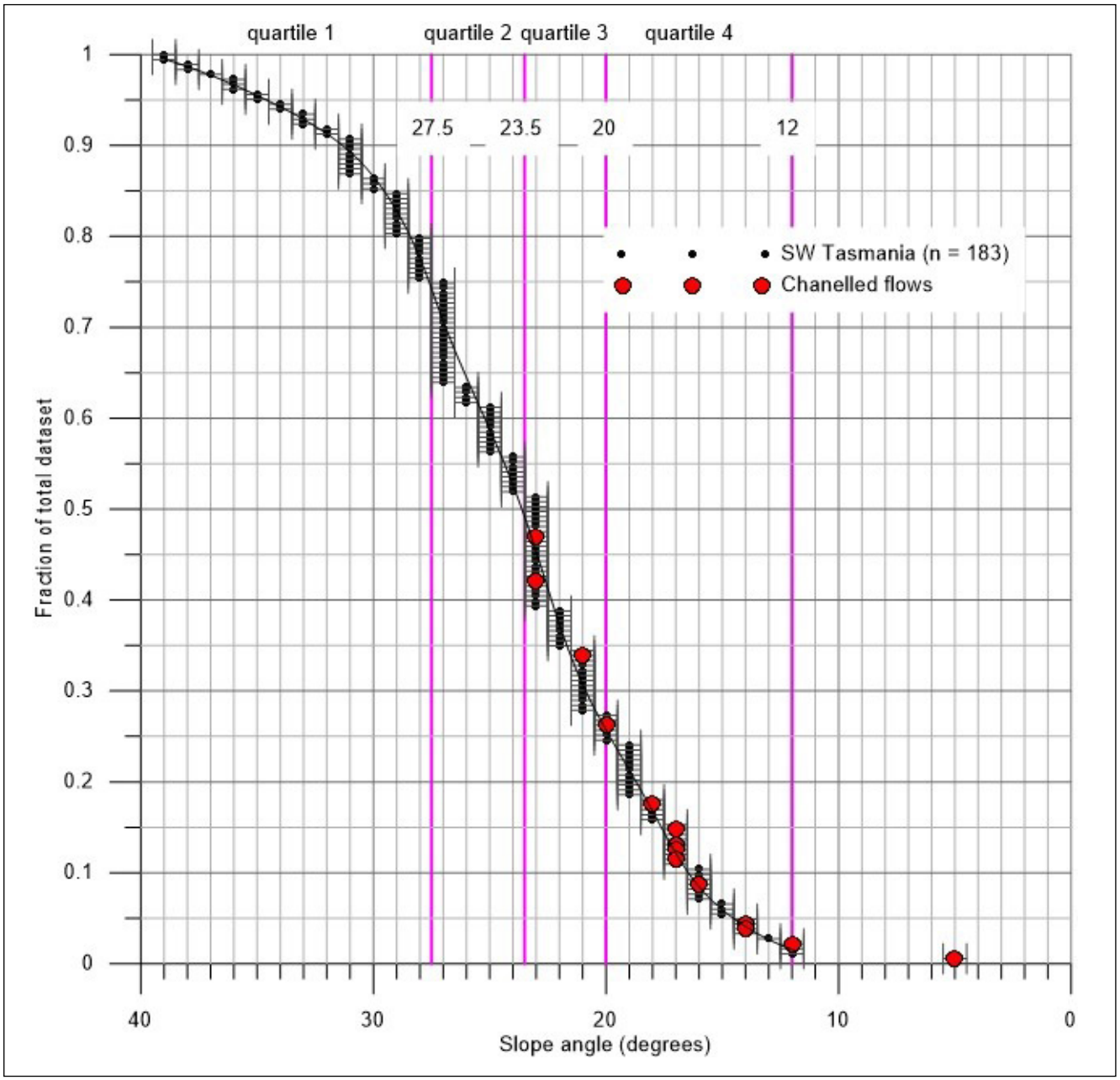

Figure 20. Distribution of debris flow travel angles SW Tasmania.

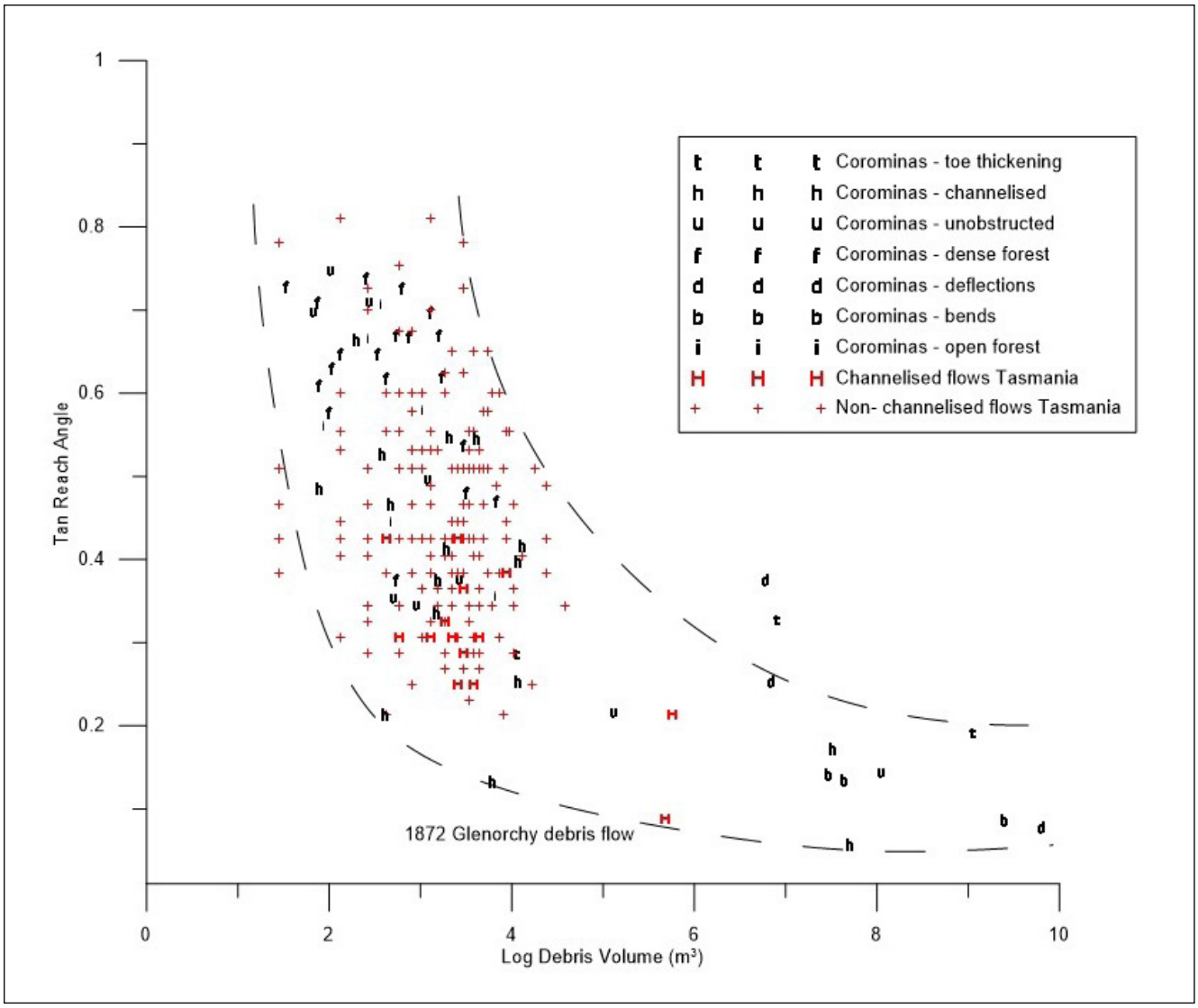

Figure 21. Comparison of a Spanish debris flow dataset (Corominas 1996) with SW Tasmania (this study).

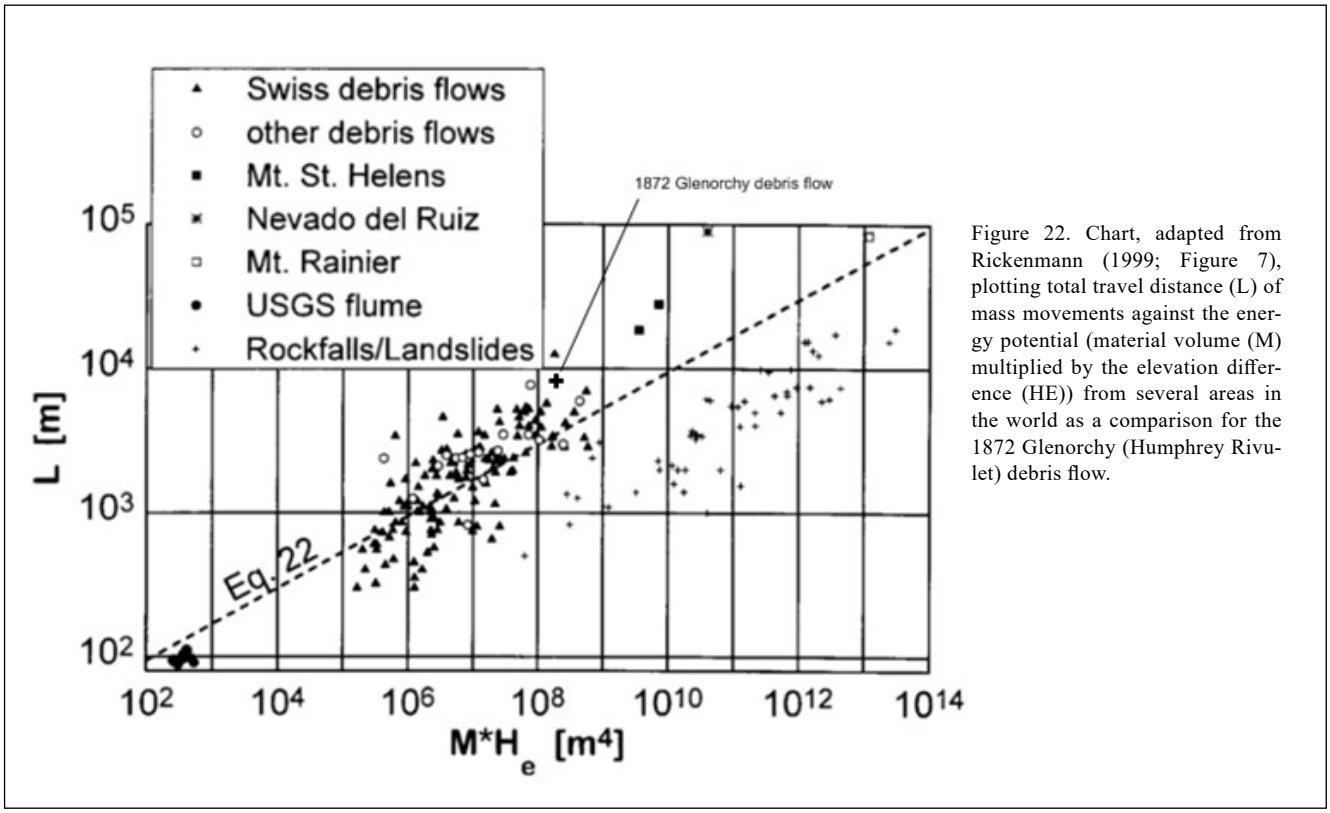

Figure 22. Chart, adapted from Rickenmann (1999; Figure 7), plotting total travel distance (L) of mass movements against the energy potential (material volume (M) multiplied by the elevation difference (HE)) from several areas in the world as a comparison for the 1872 Glenorchy (Humphrey Rivulet) debris flow.

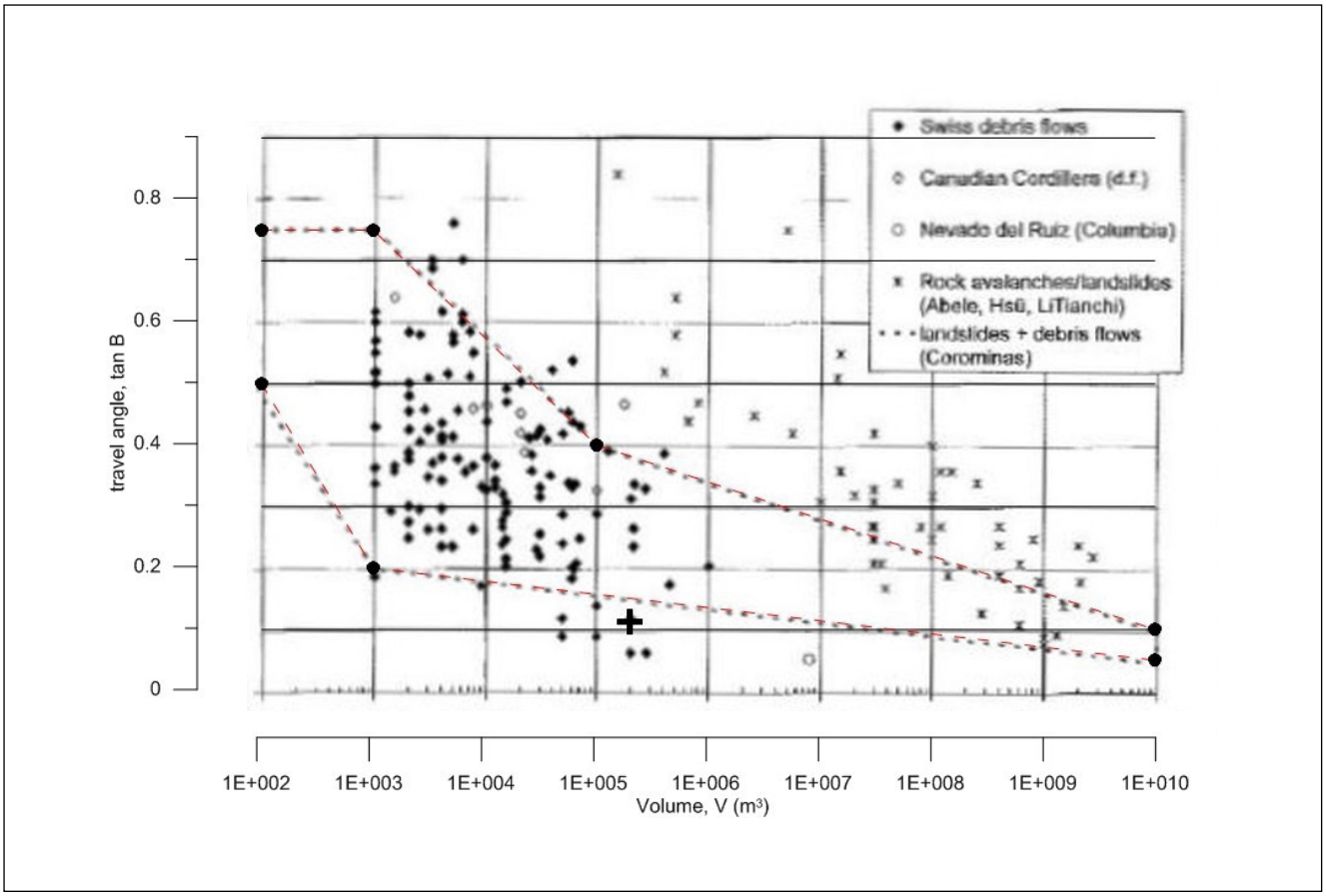

Figure 23. Chart from Rickenmann (2005, Figure 13.1) plotting travel angle against volume. Large cross symbol (lower centre-left) represents the 1872 Glenorchy debris flow.

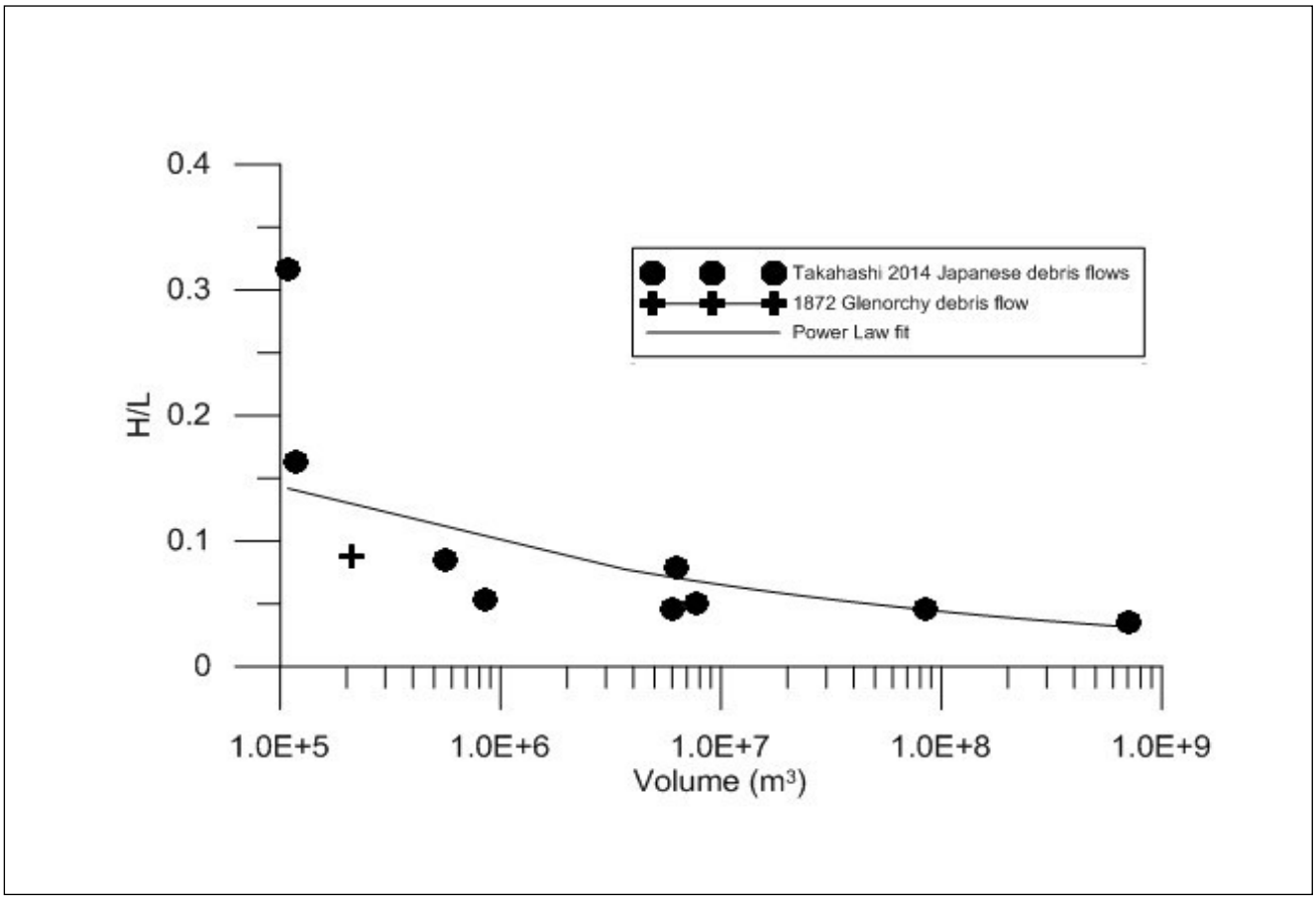

Figure 24. Volume-runout relationships for large debris flows in Japan, as described by Takahashi 2014, and including the Glenorchy debris flow.

4.4 Volume –Frequency relationships

An empirical observation in nature is that small events (such as a flood or a debris flow) occur more commonly than larger ones. Various studies on landslide datasets have, using a range of methods, established power-law relationships between volume (or area) and the frequency (or abundance) of these events (e.g. Hovius et al., 1997; Malamud et al., 2004; Moon et al., 2005; Brunetti et al., 2009 and Klar et al., 2011). The power-law relationship is particularly powerful as it has predictive capabilities when modelling the volume of an event for a given likelihood.

Table 2. Volume comparisons between previous and the current studies.

X axis approximation	Lower bin limit (volume)	Upper bin limit (volume)	Count - Fell & Moon volume estimation method	Count - this study
200	100	300	2	28
550	300	1000	31	30
2000	1000	3000	86	72
5500	3000	10000	109	65
20000	10000	30000	23	20
55000	30000	100000	6	8
200000	100000	300000	0	1
550000	300000	1000000	1	1
2000000	1000000		0	0

A power-law relationship has been established from our dataset of debris flows that have occurred in the last ~80 years using the method outlined in Moon et al. (2005). In this method, a series of logarithmic bins are created for which the count of events is recorded (Table 2). The method is essentially a histogram but displayed as a scatter plot chart from which the relationship is determined (Figure 25). The data can be divided into two parts by volume at about the 3 000 m^3 mark. The data in the upper part (larger volumes) can be interpolated as a straight line power-law, whereas the lower part does not follow this rule. For this type of landslide study the apparent non-power-law behaviour is often referred to as the roll-over effect, and may be partly explained by under-recording of smaller events in the inventory due to scale limitations of the imagery used for interpretation.

We have assumed, for the sake of simplicity, that the power-law equation in the upper part (right) can also be applied to the lower part (smaller volumes). This approach deviates from that of Moon et al. (2005) in that they progressively reduce the gradient of the line toward the left of the chart for the roll-over component based on "expert judgement". While neither method is particularly rigorous, it makes very little difference as it is the larger volume flows which matter most in predicting potentially destructive events.

The established power-law relationship provides a means of estimating the geomorphic process rates for debris flow over a historical period of time that, with additional factors, can be used as a predictor of the future events.

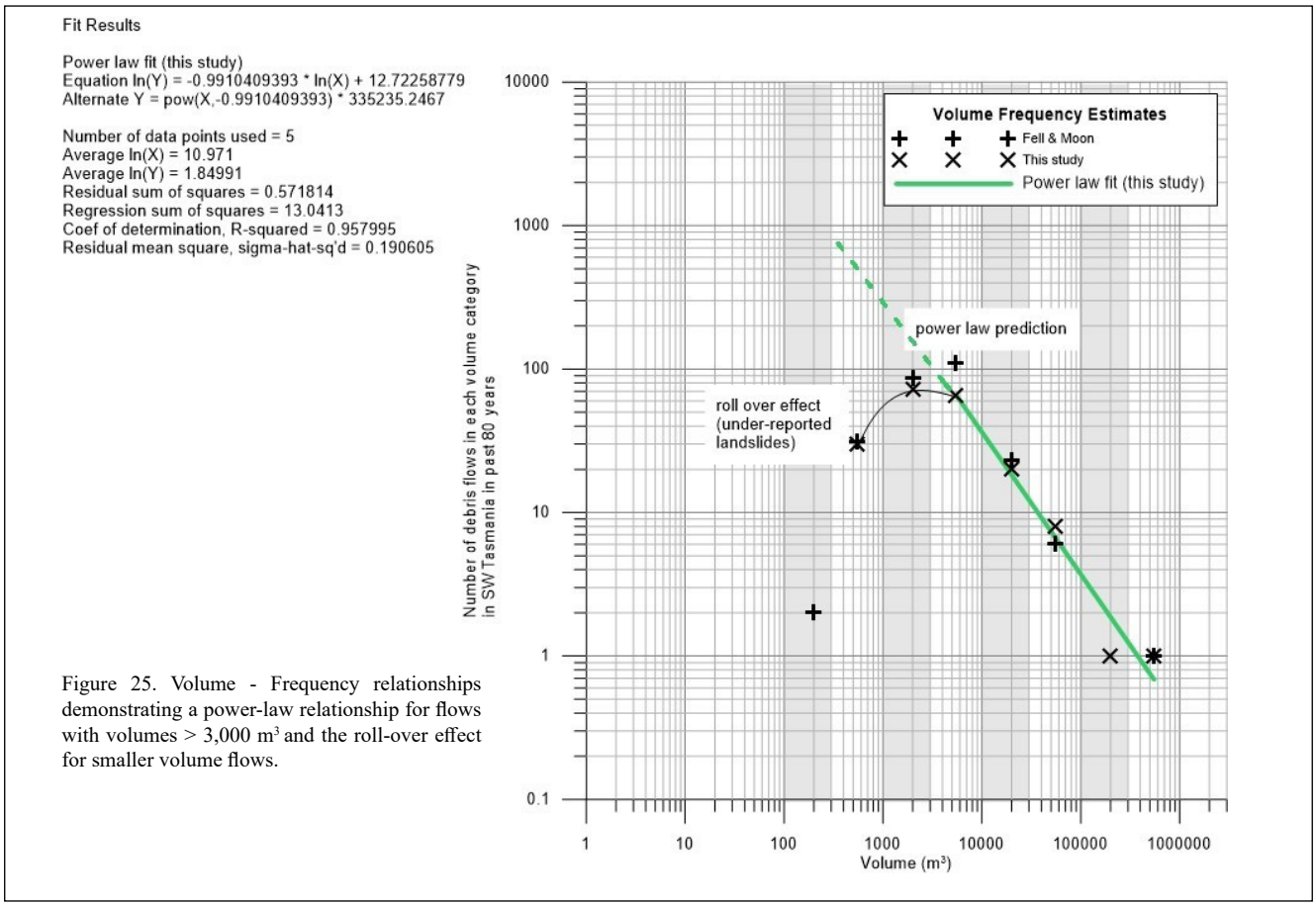

Figure 25. Volume - Frequency relationships demonstrating a power-law relationship for flows with volumes > 3,000 m^3 and the roll-over effect for smaller volume flows.

However, the limitations to this approach should be noted:

- Given that our database is substantially the result of only a few low probability rainfall events, a longer record of past events may produce a different power-law relationship. We note that the trigger rainfall for the 1872 Glenorchy Debris Flow was estimated as a slightly less than 1% event and that antecedent rainfall played little part in the event (Stevenson et al., 2016).
- Given that the Bureau of Meteorology 2016 Intensity Frequency Duration (IFD) estimates of extreme rainfall events varies across Tasmania, a prediction for a specific part (i.e. kunanyi / Mount Wellington) will at best be an averaged value. However, a brief inspection of two points representing the northwest and sothwest extents of the regional study area compared to kunanyi / Mount Wellington (that sits significantly to the east) indicates that the rainfall estimate in the southwest area is quite similar for the 1:100 year (1%) probability. In contrast, the northwest IFD has significantly lower rainfall values. As most of the landslide data comes from the southest and kunanyi / Mount Wellington areas this is somewhat encouraging and suggests that the averaging effect will have little impact on the landslide tempo.
- The impact of predicted climate change on the estimated tempo has not been considered and is beyond the scope of this report.
- Future changes to forest cover (e.g. as a result of bush fire, land use changes and climate change) have also not been considered.

5.0 SUSCEPTIBILITY MAPPING

The goal of achieving a design event (volume) prediction for a debris flow simulation, in a similar manner to flood modelling, requires the power-law distribution (based on a finite number of events), to be normalised into an annualised form (assuming an 80 year record) and to be further normalised against the areas of deemed susceptibility. This can be considered as a regional geomorphic process rate per unit area. Design event volumes, for a given catchment, are then calculated by multiplying the area of deemed susceptibility by the rate/area value.

The susceptibility determination is therefore divided into two parts:

- a regional study comparing similar geology and geomorphology to kunanyi / Mount Wellington that provides us with a statistically significant landslide dataset and;
- a local study focused on kunanyi / Mount Wellington itself.

Because of computational limitations, the size difference between the two areas has meant that different tools were used in each case. However, we have assumed that any differences in method are minor and will not significantly affect the overall prediction.

5.1 Regional Susceptibility

Within the regional study area (SW Tasmania), most recorded landslides are situated on steep terrain that comprise a relatively small proportion of the area. We have analysed our inventory by considering the slope and contributing hydrological area for the source region of each feature. While other factors, especially geology, are important for susceptibility mapping, the most detailed geological layer for much of the area is compiled at 1:250 000 scale and is known to have significant reliability and accuracy issues. For this reason we have not used this layer in our analysis.

Our approach for choosing the appropriate parameters of slope and contributing area has been to maximise the prediction rate for our database (Figure 26) while minimising the area of susceptibility. This is displayed where we have identified a “sweet spot” (slope of 17^0 and area 10 m^2) as our minimum thresholds (Figure 27) to produce a regional susceptibility map (Figure 28). Our calculations are provided in the following table (Table 3) and the derived 66.3 km^2 value is used to normalise the magnitude-frequency chart.

Table 3. Summary of debris flow susceptibility parameters in SE Tasmania.

Regional study area	3599 km^2
Susceptible area	66.3 km^2
Proportion of regional study area deemed susceptible	1.8%
Total number of landslides	374 (~80 years and older)
Number of landslides predicted	365
Landslide success rate	97.6%

5.2 kunanyi / Mount Wellington susceptibility

5.2.1 Source areas

We have revised the susceptibility mapping on kunanyi / Mount Wellington from the previous work of Mazengarb (2005) with the benefit of acquired experience, a superior LiDAR-based DEM, refined mapping, and by utilising software tools that have recently become available.

The first generation debris flow susceptibility maps of Hobart and Glenorchy determined source areas using the GIS utility Shalstab (Dietrich and Montgomery, 1998) and described in Mazengarb (2005). Unfortunately this software no longer works in more recent versions of ESRI GIS software. Subsequently, a similar programme called SINMAP (Pack et al., 2005) was de-

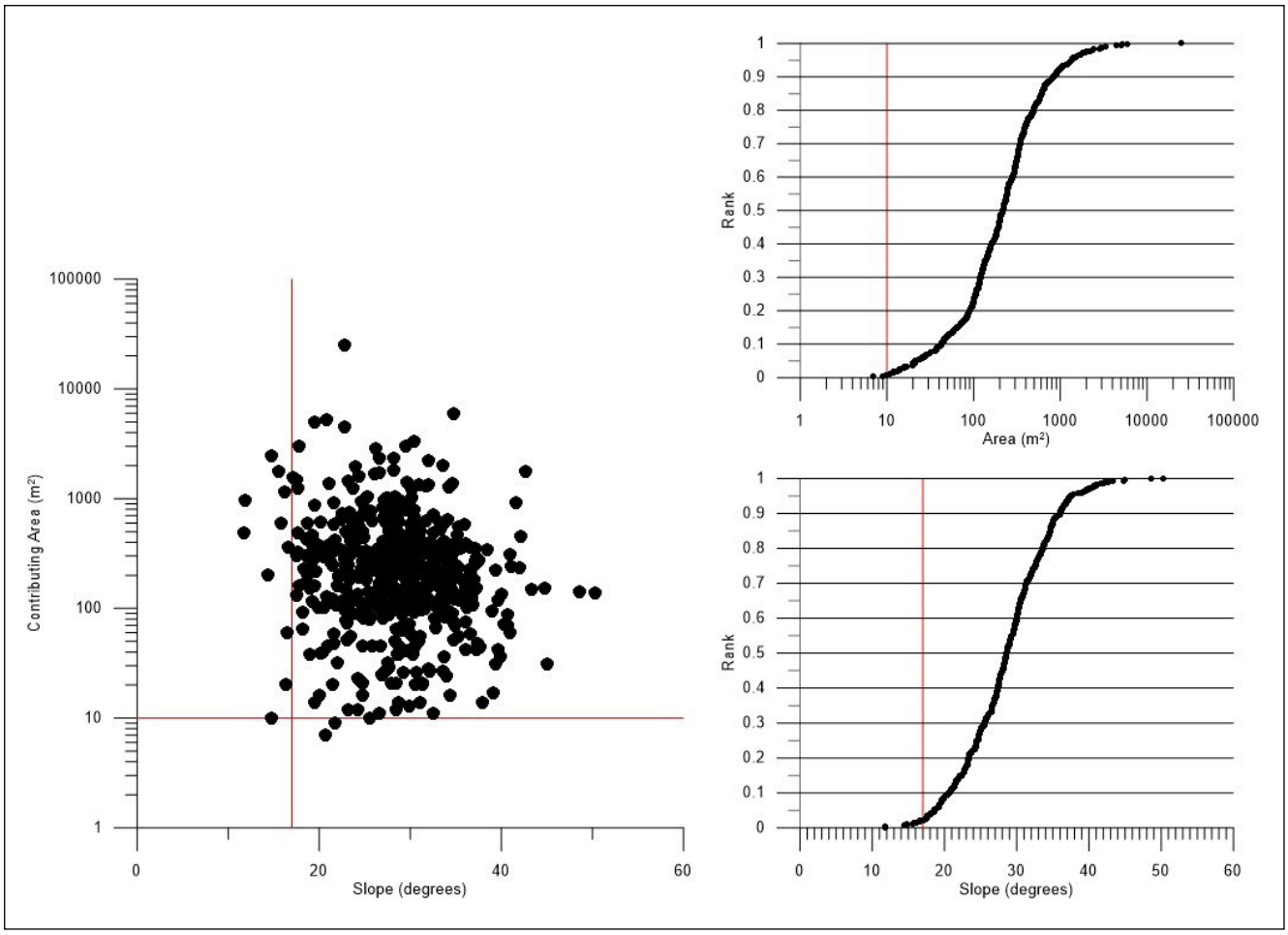

Figure 26. Statistical analysis of slope and contributing hydrological areas for debris flows in the regional study area. Red lines indicate chosen thresholds for the susceptibility model.

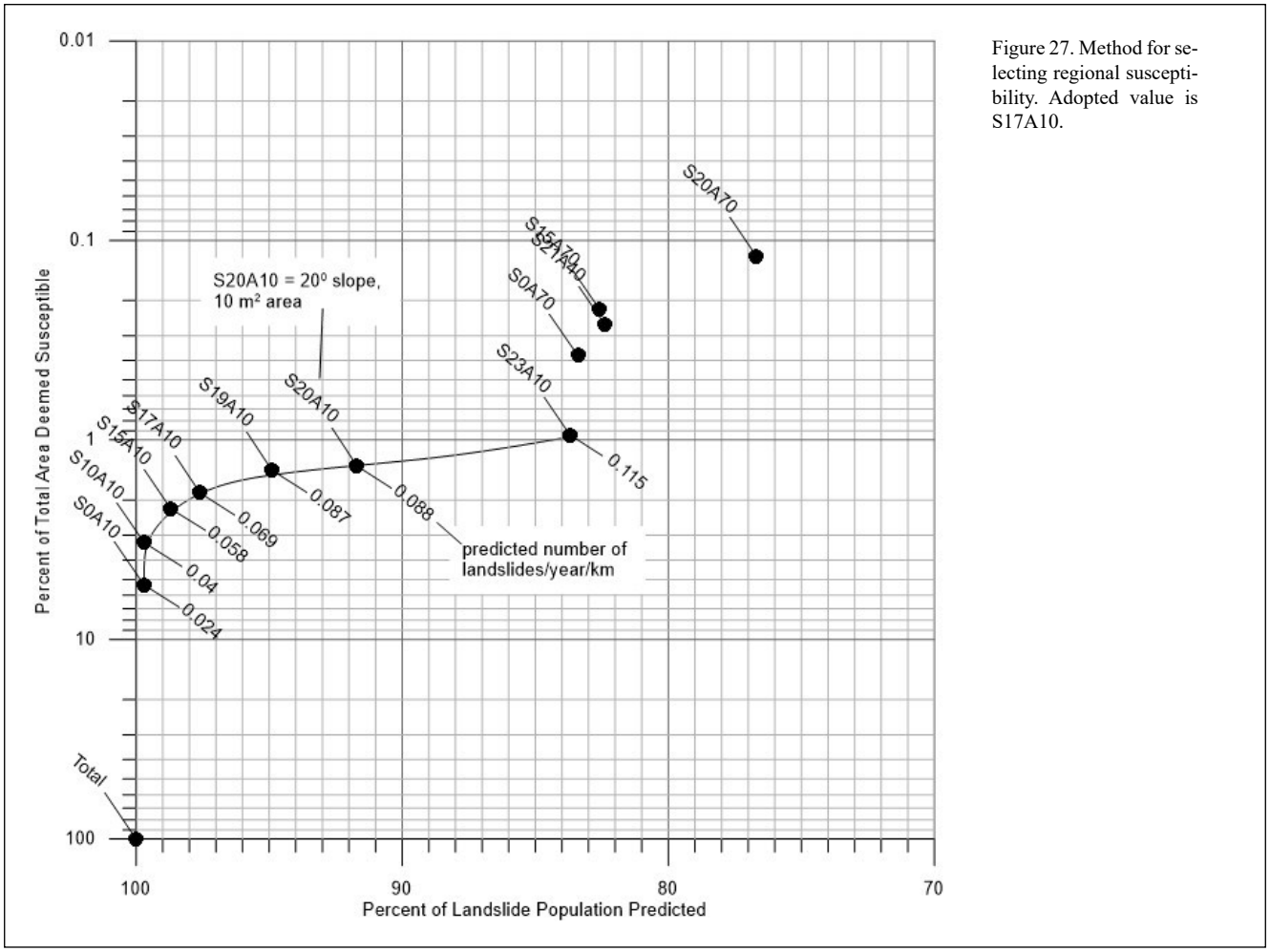

Figure 27. Method for selecting regional susceptibility. Adopted value is S17A10.

veloped for an ESRI GIS environment which also combines steady-state hydrologic concepts with the infinite slope stability model. A detailed discussion of the differences in approach to Shalstab is provided in Pack et al. (2005). Alas, SINMAP version 2 has suffered a similar fate to Shalstab and we used a more limited version available in MapWindow (a Free and Open Source GIS program). We note that the algorithms are also available in the SAGA software package.

SINMAP provides tools for rapid calibration of our landslide database against the model predictions that have been particularly useful. The methodology relies on the following inputs and parameters:

1. A 10 m DEM constructed from the 2011 Mt Wellington LiDAR acquisition. The cell size chosen is considered, based on a number of studies, as an applicable value for regional studies.
2. A dataset of shallow landslide source points with each point positioned in the head of the landslide to be representative of the general slope and reflect the hydrological contributing area.
3. A polygon layer representing the areas where we believe significant surficial material including weathered bedrock is available that could potentially fail and in which almost all of our mapped shallow landslides lie. This layer is based substantially on the published 1:25 000 geological map by MRT with minor modifications as a result of mapping for this project.
4. SINMAP input parameters chosen to achieve the adopted source area are provided below. In contrast to the SHALSTAB method, certain input parameters are entered as ranges, not single values.
    - T/R lower bound 2000
    - T/R upper bound 2800
    - Cohesion lower bound 0.01
    - Cohesion upper bound 0.12
    - PHI lower bound (degree) 23
    - PHI upper bound (degree) 40
    - Soil density (kg/m3) 2000
5. We have chosen, for the sake of simplicity, to adopt all Stability Index values <= 1 (this is roughly equivalent to a factor of safety value) to act as source cells for subsequent runout modelling.

The SINMAP approach employed in this study successfully predicts about 93% of our landslide population in 70% of the area where we consider geological materials capable of failing occur (Figures 29 and 30).

5.3 Regional scale runout modelling

The previous generation of debris flow mapping in Hobart and Glenorchy (Mazengarb, 2004a, 2004b) used a simplistic runout method developed by the senior author (Mazengarb, 2005) in the absence of a ready-made product. Since then, runout simulators of varying sophistication have become available and we have used Flow-R (Horton, et al., 2013) to repeat this work. Flow-R is a raster-based simulator for debris flow and other gravitational slope processes developed at the University of Lausanne that offers a greater level of sophistication than the runout model used previously. In this study, we have performed a number of simplistic simulations to determine what we consider to be a best fit solution (Figure 31). It is recognised that further levels of sophistication, which consider factors such as forest cover and land use, are possible with this software, and while we agree incorporating these factors t would be beneficial in the near future, they were considered beyond the scope of this study.

The parameters chosen are:

Calculation Method: Quick: energy based discrimination (recommended)

Spreading Algorithms:

Directions algorithm: Holmgren modified Dh=2m exp=1

Inertial algorithm: Weights method, default

Energy Calculation:

Travel Angle limit: 12

Velocity: limited to a maximum of 15 m/s

We chose the Quick method based on the recommendations contained in the software. The spreading algorithms consider an allowable height of the flow in the channel, the value of which (Dh = 2 m) was chosen as a somewhat arbitrary but realistic figure. The exponent parameter (exp) controls the dispersion of the flow that, in combination with Dh, produces a smooth buffered zone around channel margins and curved travel lines (reflecting slope direction) on the hillsides above. Significantly higher values of the exponent produced unrealistic straight line travel paths on the hillsides. The travel angle value was chosen to match the statistical distribution of our regional dataset discussed previously whereas the velocity limit was a somewhat arbitrary choice.

Our indicative susceptibility map (Figure 31) is considered an improvement on the previous work for several reasons, including the probabilistic approach that assists risk assessment methods and that it honours the recommendations of the Fell and Moon (2007) report; particularly the limiting of runout but increasing

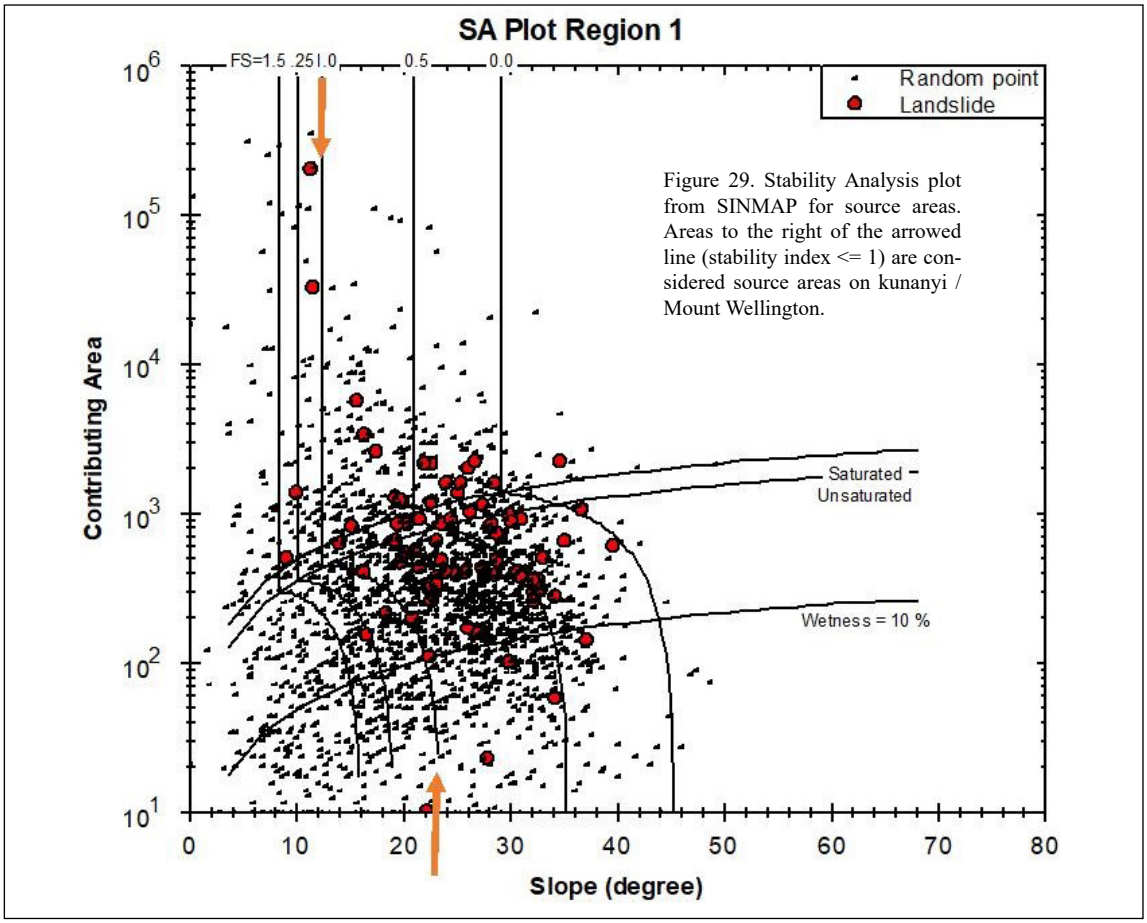

Figure 29. Stability Analysis plot from SINMAP for source areas. Areas to the right of the arrowed line (stability index <= 1) are considered source areas on kunanyi / Mount Wellington.

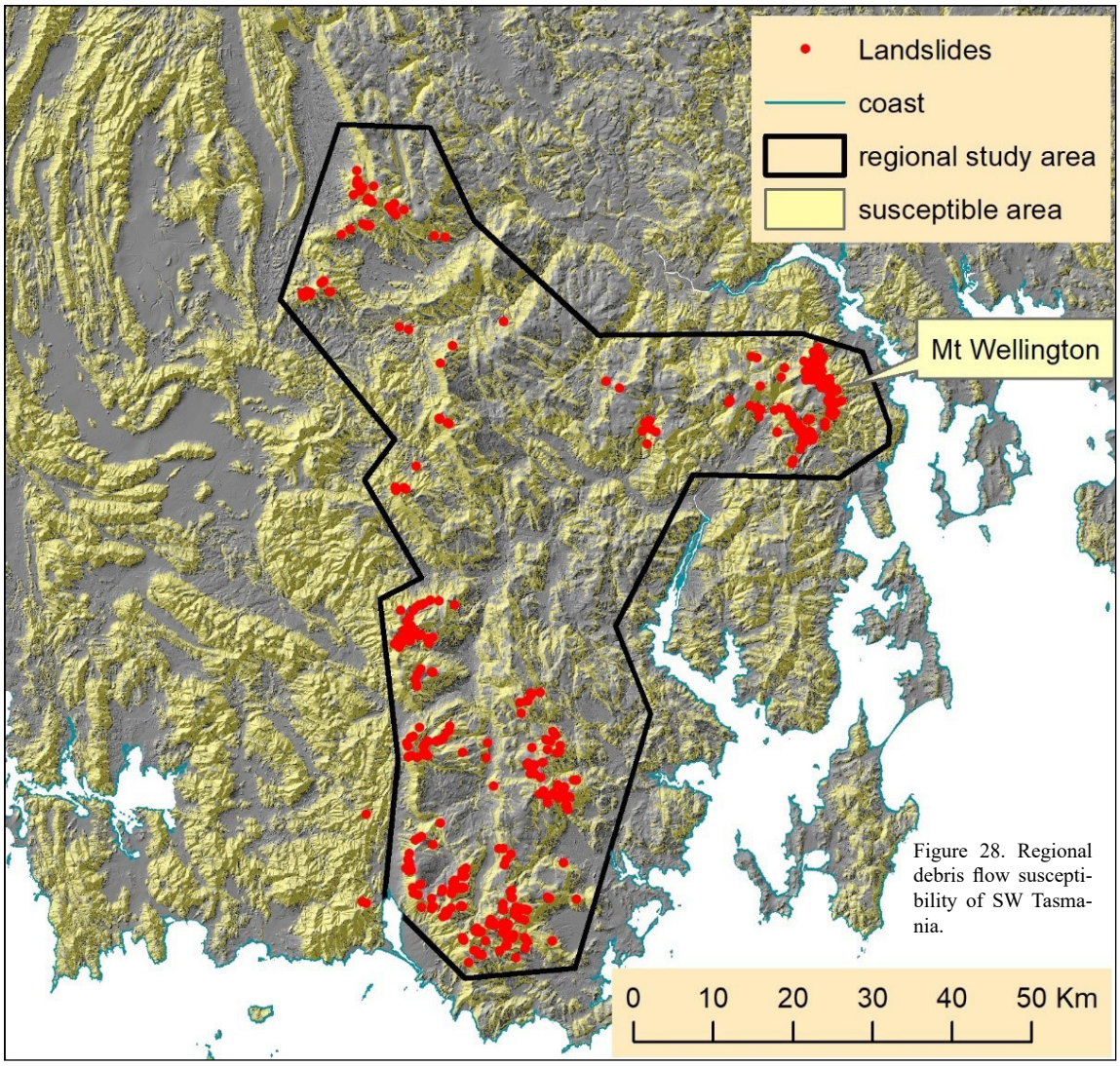

Figure 28. Regional debris flow susceptibility of SW Tasmania.

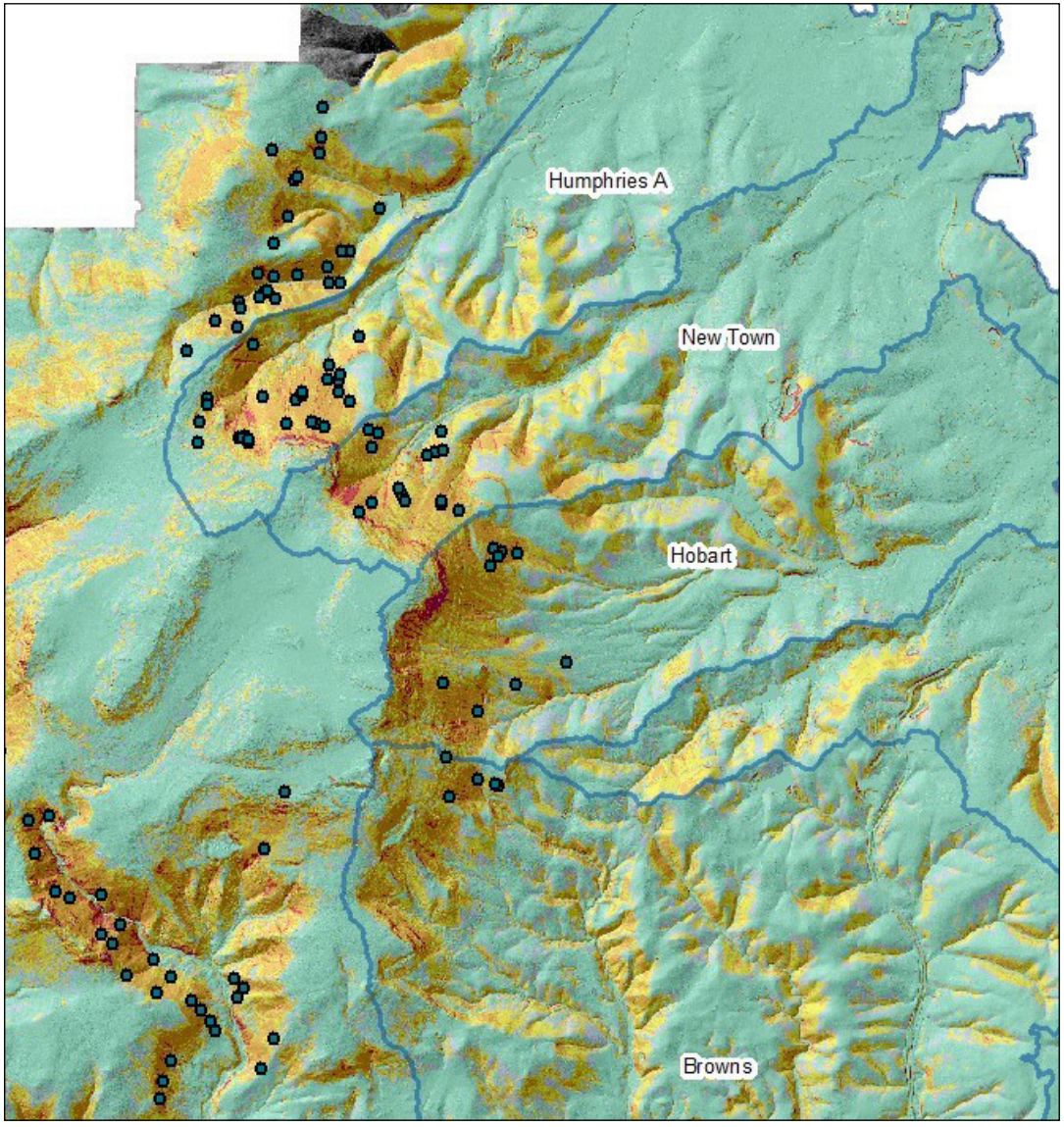

Figure 30. Calculated SINMAP stability classes showing the catchments under consideration. Darker brown to red colours indicate higher susceptibility.

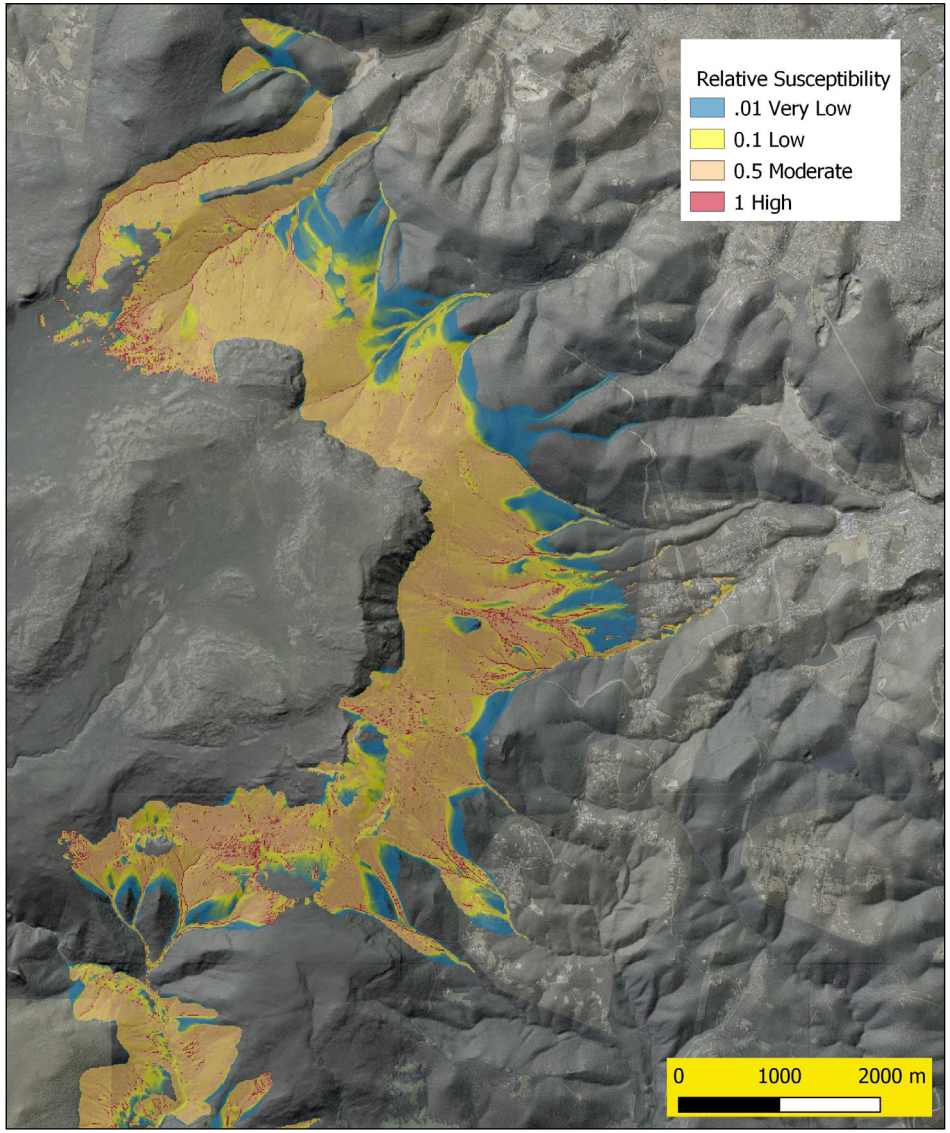

Figure 31. Probabilistic debris flow susceptibility map calculated using Flow-R software.

the areas where potential failures could originate. The Flow-R model predicts that much of the upper slope is susceptible to debris flow runout which is consistent with our mapping of surficial deposits and debris flow features. Many of the flows reach defined channels as would be expected and this is where the highest probabilities occur. As discussed above, there is uncertainty as to how likely debris flows would initiate on the forested parts of the slopes (rather than gully heads or channels) in our present warm climatic conditions. Fortunately these areas are generally well away from fringing settlements so the discussion is not critical, but should forest cover alter over time (e.g. as a result of fires) this may need to be revisited.

The most significant limitation of the Flow-R model is that does not readily explain how the 1872 event seemingly behaves in a different manner to typical debris flows. In our view Flow-R is well suited for regional scale applications but when considering more site specific analyses other tools that are able to model fluid flow with a range of rheological properties, and that factor the volume of material involved for a given flow scenario, are probably better suited.

5.4 Site specific runout modelling

5.4.1 Software capability and limitations

Modelling of debris flows is far from a mature science. Many software approaches have been developed over the last two decades, with varying levels of sophistication and widely ranging capabilities. All are based on a number of simplifying assumptions and there is ongoing research to develop computational tools to replicate these complex processes (e.g. Rickenmann, 2016). We therefore urge caution in interpreting the models presented in this report, and consider that the results are only one of many possibilities with parameters chosen as a result of limited calibration and professional judgment. We suggest that our results be considered indicative, rather than absolute, and that any implementation in terms of risk management be mindful of the inherent limitations of the modelling.

For the sake of brevity, several software options were considered at the beginning of the project, both open source and proprietary. MRT initially purchased Flo-2D, as at the time in 2013 it was considered by us to be the best choice based on several criteria (including affordability). Flo-2D is underpinned by a considerable amount of fundamental research (e.g. Rickenmann, 2016) and while some successful testing of the software was undertaken in our study there were several issues that arose that limited the utility of the programme.

However, an alternative software solution River-Flow-2D (RF-2D) was also used as it includes a Debris Flow Module and has computational advantages and improved versatility. RF-2D performs two dimensional finite-volume fluid dynamics in an unstructured grid/mesh processing architecture compared to the raster environment of Flo-2D. Recent developments include integration within a standard GIS environment (QGIS) for pre- and post- processing functions that makes it a more comfortable environment for users with GIS skills; and its ability to utilise GPU hardware for improved performance.

Debris flow software such as RF-2D contain a variety of parameters to control the rheological properties of the flow (Table 4). In addition it can perform either dry-bed or wet-bed simulations and takes into account the effects of surface roughness to the flow.

Table 4. Rheological model options and their user-defined parameters in RF-2D.

Mechanism	Yield Stress	Viscosity	Cv (sed. conc.)	Internal friction angle	Material density	Manning's n
Turbulent					Yes	Yes
Full Bingham	Yes	Yes	Yes		Yes	Yes
Simplified Bingham	Yes	Yes	Yes		Yes	Yes
Turbulent and Coulomb				Yes	Yes	Yes
Turbulent and Yield	Yes		Yes		Yes	Yes
Turbulent Coulomb and Yield	Yes		Yes	Yes	Yes	Yes
Quadratic	Yes	Yes	Yes		Yes	Yes

At the time of running the simulations for this report, the software assumes that the rheological properties are constant throughout the simulation (i.e. no variation in rheology with solid/water variations during the event). This is of concern and is a recognised limitation, in that testing by many researchers (e.g. Iverson, 2003) has demonstrated that viscosity and shear strength may vary across orders of magnitude as Cv (sediment concentration) varies from 45 to 65% during a single event. Furthermore, the software does not consider entrainment (scour) of coarse material encountered, nor deposition along the path of the flow.

Notwithstanding these limitations, they are not as important as concerns arising from:

- the impact that the chosen rheological model can have on flow behaviour given difficulties in rationally choosing the most appropriate model;
- the uncertainty that arises from the major disparity between laboratory or field back-calculated viscosity and shear strength and similar values derived by model calibration to actual event data.

Current investigations into flow resistance are focused on relationships that could best represent a debris flow

in the mid-range of Cv's, notably: Simplified or Full Bingham, Turbulent and Yield, Turbulent Coulomb and Yield and Quadratic methods. It is from these methods that we have undertaken our runout modelling.

5.4.2 Model Calibration

In our study we used our mapping of the 1872 Glenorchy Debris Flow as a primary means of calibrating the parameters used in RF-2D for the kunanyi / Mount Wellington catchments. We have also considered the 1960 New Town Rivulet debris flow in our calibration exercise for comparison, although its former extent is less constrained and not as reliable (Figure 32). We have also undertaken a calibration of the other large feature in our dataset, in Judds Creek, where we have a very good photographic record of its extent (Appendix 2).

5.5 Humphreys Rivulet, 1872 Glenorchy Debris Flow Event Validation

A RF-2D model has been constructed using catchment conditions as existing in 1872 and the model was run for a range of debris flow volumes and material properties. The following preparatory steps were taken:

- Building a 5 m resolution DEM to replicate the 1872 landscape. This was based on using a LiDAR derived DEM that was converted to closely-spaced contours and then interpolated back to a DEM using the TopoToRaster function in ArcGIS. The reason for undertaking this step is that this method allows the easy removal of many post-1872 cultural features (e.g. road embankments, quarries) through the use of exclusion polygons.
- Creating a likely Mannings-n layer for 1872 landscape based on general descriptions contained in the historical record.
- Creating a processing mesh (triangular) of various resolutions down to 5 m in the area of interest within RF-2D within a defined domain area.
- Placing an input source point at the most likely location for the debris flow with an associated discharge vs time file. A volume for the event had been previously estimated (Stevenson, et al., 2016) and a somewhat arbitrary value of 60 seconds chosen for the discharge to occur that is consistent with known discharge rates in Rickenmann (1999).

The range of parameters explored for Humphreys Rivulet are indicated by the two grey limit lines plotted in (Figure 32) and assuming a volume of 200,000 m^3 in all cases. A best fit was found to the historical record in terms of extents and indicative timing using the following parameters:

Flow resistance relation: Quadratic (e.g. Naef, et al., 2006)
Yield stress (N/m^2): 100
Viscosity (Pa*s): 50
Cv: 0.1
Internal friction angle (degrees): 3.5 (preset value)
Flow material density (kg/m3): 1400

As is evident in Figure 33, these properties are consistent with a relatively fluid flow as would be expected under the conditions prevailing in the catchment at the time of the event. The low Cv value used here, taken at face value suggests this is a hyper-concentrated flow rather than a true debris flow. However, given the fixed rheology limitation of the software discussed previously, we argue that a range of flow conditions may have existed at different stages of the event for various reasons. For instance, it is possible that some of the heavier material may have dropped out of suspension once the flow began to slow when it reached the lowland near Tolosa, but the water would continue moving downstream regardless along with the timber floating in it. This would match the historical record wherein Stevenson et al. (2016) identified the likely transition from a debris flow to a hyper-concentrated flow on the lower floodplain at Glenorchy, involving the transport of large logs and considerable mud to the Derwent Estuary. Another factor identified in Stevenson et al. (2016) is that the debris flow occurred at the end of a large rainfall event that saw Humphrey Rivulet in full flood, although the flood had been subsiding gradually up to the time of the debris flow. This flooding is likely to have introduced significant water into the flow once it reached the floodplain. While we can discuss the semantics of the flow itself, it would be highly hazardous none-the-less.

A more viscous flow, matching the definition of a true debris flow (with much higher Cv), would not have travelled as far and would have taken a much longer travel time as evidenced in our experimental simulations. This is the basis for the Fell and Moon (2007) conclusion discussed previously and why they invoked a second phase debris dam breach to explain the greater extent of the historical event. While we cannot, and should not, dismiss their hypothesis entirely, we suggest that our model provides a much simpler explanation that is in accord with the assessment of the historical observations (Stevenson, et al., 2016) and consistent with the debris flow occurring at a time when Humphrey Rivulet was already in flood.

A comparison of the historical extent, as mapped in Stevenson et al. (2016), and the runout model is presented (Figure 34) and indicates a relatively close match given the various inherent uncertainties. A comparison

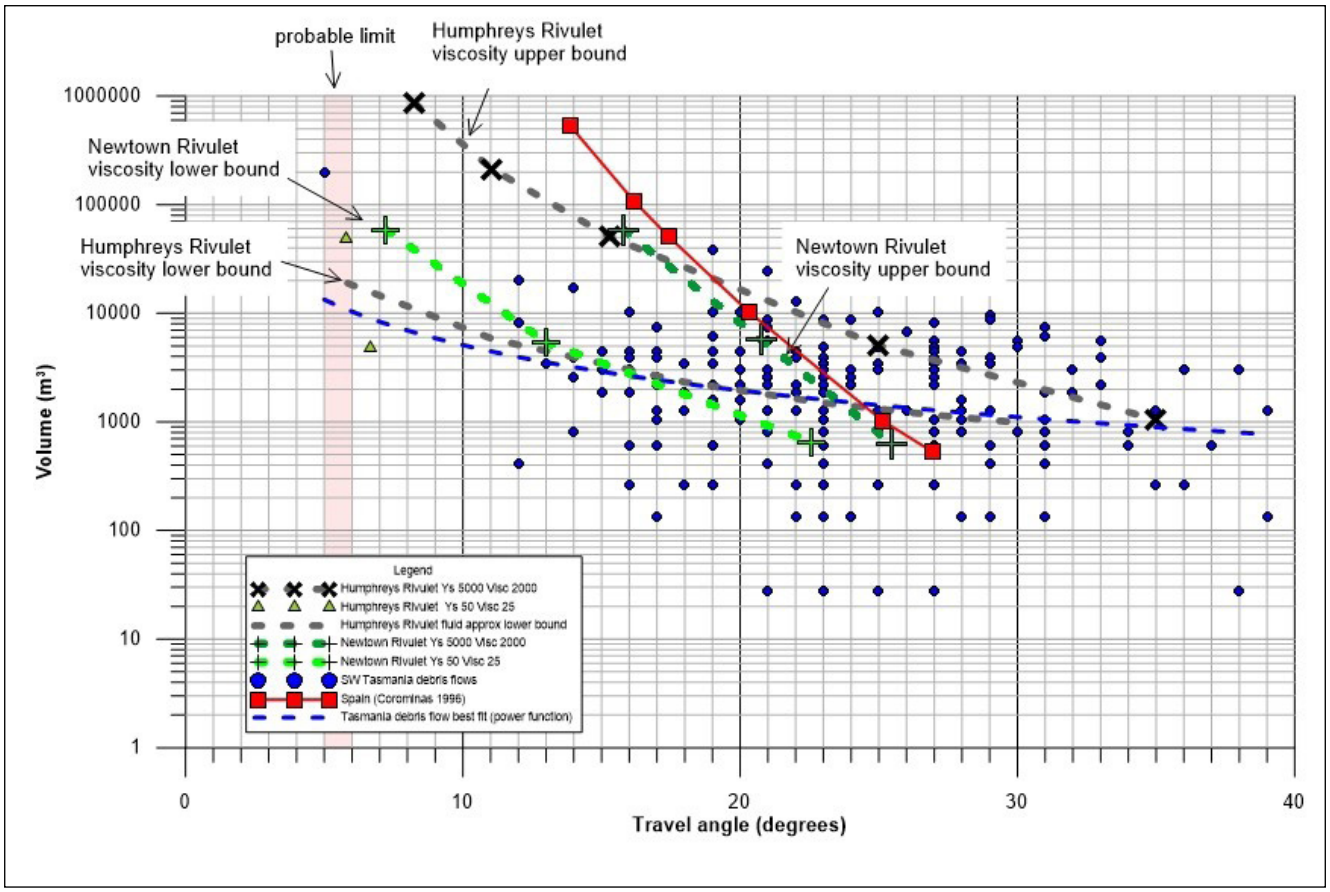

Figure 32. Calibration of RiverFlow-2D debris flows rheology parameters against empirical constraints.

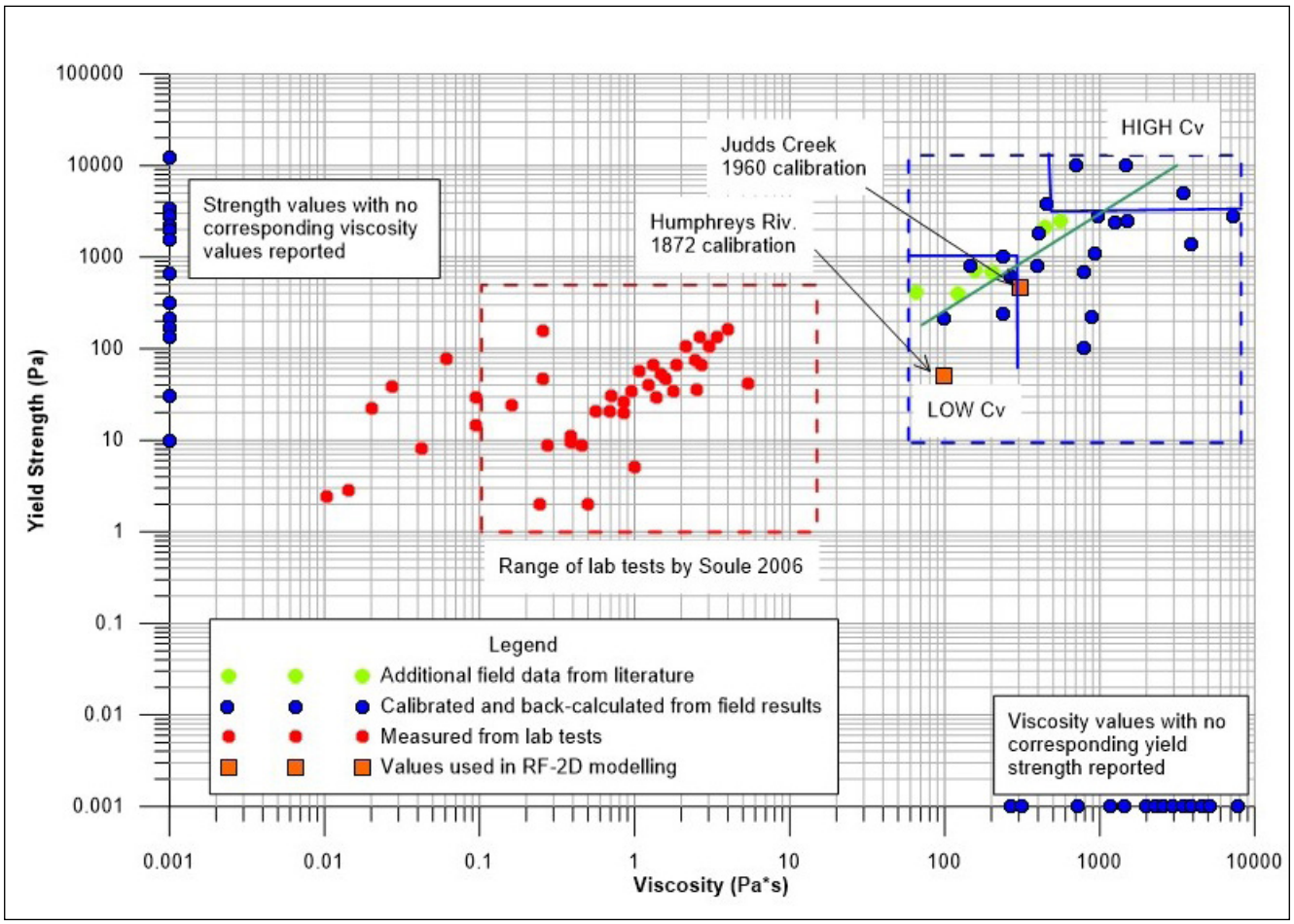

Figure 33. Rheological properties of debris flows based on a chart by Prochaska et al. 2008. Cv zones as defined by Whipple and Dunne 1992. Values modelled for the Humphreys Rivulet and Judds Creek debris flows are shown.

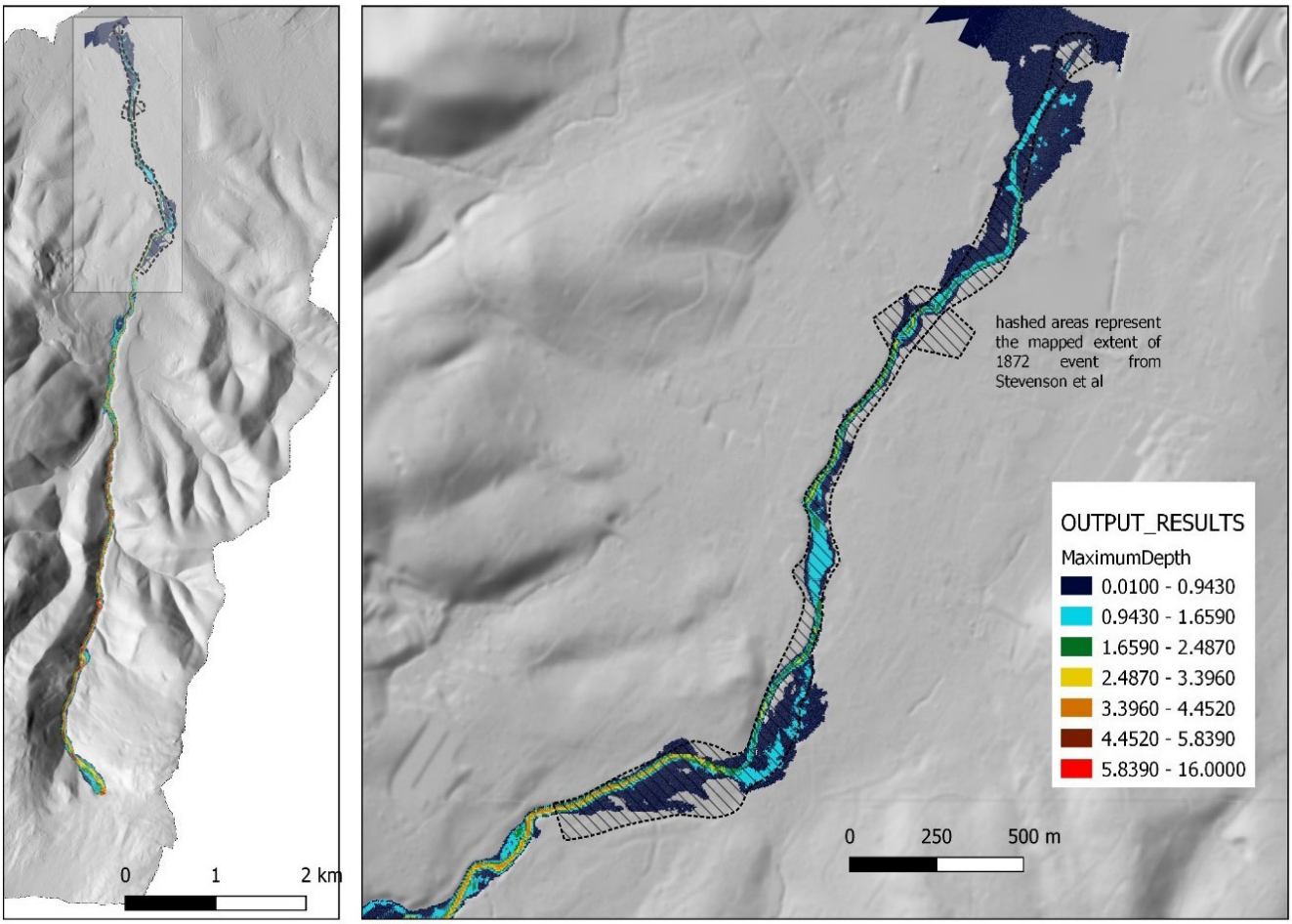

Figure 34. Modelled 1872 Glenorchy Debris Flow with historical control.

was also undertaken to compare the effects of a modern (2011) terrain and Manning's n model that shows that the more recent cultural changes to the landscape have made surprisingly little difference (Figure 35).

A calibration of the Judds Creek landslide (the largest by volume debris flow in our regional dataset) is presented here to compare the likely rheological properties (as determined by model simulations) with the Humphreys Rivulet event. A description of the Judds Creek feature is provided in Appendix 2 based substantially on aerial photograph interpretation and LiDAR imagery. Our analysis of the event demonstrates the inherent complexity of the feature, with most of the material (~300-500 000 m^3), travelling only a short distance (about 200 m) whereas a small component (~20 000 m^3) travelled much further, about 1300 m distance. We have chosen to model the later part of the flow only.

The calibration exercise indicated that the rheological properties to the 1872 Glenorchy Debris Flow are not appropriate at Judds Creek. Instead a Full Bingham model with substantially different parameters was chosen to significantly limit the flow extent. The choice of values for yield stress, viscosity and sediment concentration were based on the equations provided for laboratory measurements of the Aspen natural soil (O'Brien and Julien, 1988), a mud dominated material provided as an option in RF-2D. Because yield stress and viscosity are exponentially related to Cv, the sediment concentration was adjusted from a low value successively upwards until an approximate match was established between observed and modelled extent.

Above Cv = 0.54 the flow is markedly restricted in extent as viscosity and yield stress become significantly larger. Experiments with dry bed and wet bed (1 m deep) conditions showed little difference.

Parameters chosen for the Judds Creek simulation:

Flow resistance relation: Full Bingham

Yield stress (N/m^2): 306

Viscosity (Pa*s): 468

Cv: 0.53

Internal friction angle (degrees): 3.5 (preset value)

Flow material density (kg/m^3): 1874 (using default source material density of 2650)

It is noted that the simulation was performed on a modern LiDAR based DEM that was not the same as the 1960 landscape due to the difficulty of removing any changes that happened in the landscape during and after the event. However, the results show remarkable similarity to our mapping (Figure 36) especially at the two tributaries where debris dams were formed and further

Figure 35 (above). Comparison of runout models using 1872 and 2011 landscapes.

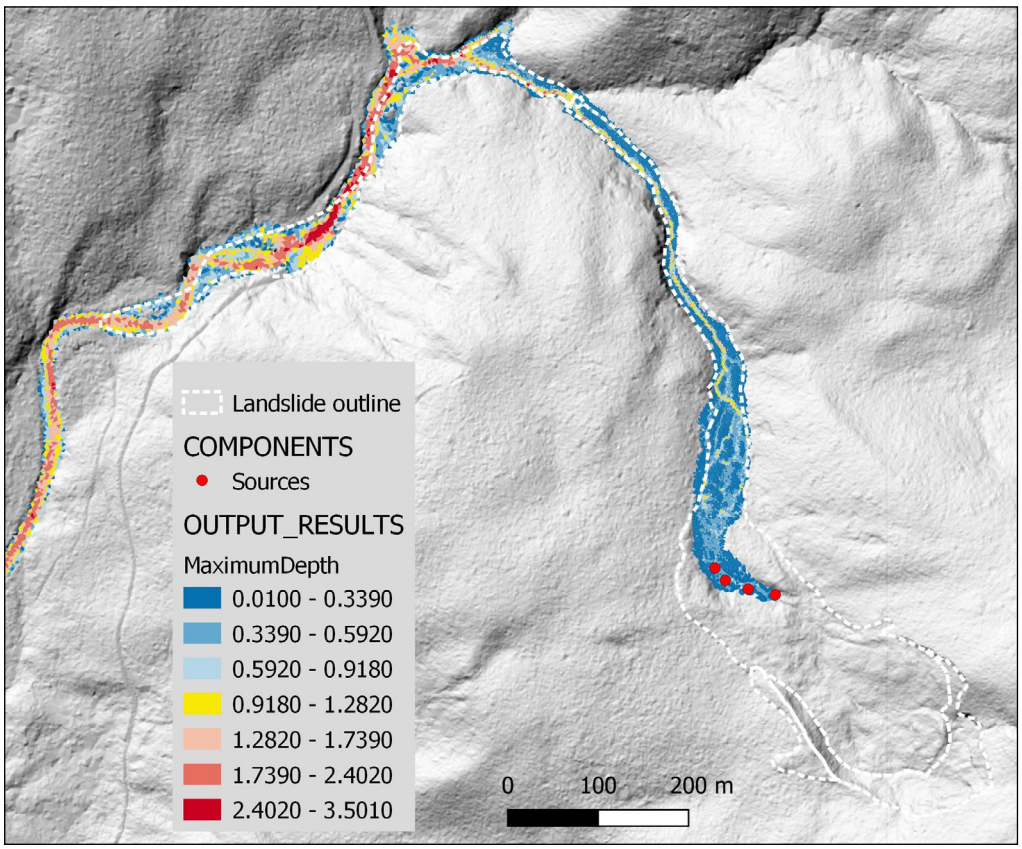

Figure 36 (left). Debris flow runout simulation for lower part of landslide.

downstream. It is noted that the modelled flow continues in the channel beyond the mapped limit of the flow (and also beyond the model domain where the colours stop). This may reflect the difficulty in mapping the true extent of the feature given the nature of the available evidence (Appendix 2).

5.6 kunanyi / Mount Wellington sub-catchment simulations and outputs

In this study we have determined volume – likelihood relationships to be applied for specific scenarios in four sub-catchments (listed below) on the mountain. Note that part of Humphreys Rivulet (the Knights Creek tributary catchment) has not been considered in this study as it is currently dammed by a reservoir and are making an assumption that this asset is well managed by its owner, TasWater.

Susceptible areas for each catchment (i.e. areas where debris flows might initiate) calculated previously using the SINMAP method were each divided by the regional area deemed susceptible in SE Tasmania to determine the fractional area. These values were then multiplied against the regional volume-likelihood curve to create a unique catchment curve (Figure 37).

From these catchment specific curves, four design events have been modelled, representing annual probabilities of 1:100, 1:500, 1:1 000 and 1:2 000. These models have used the 1872 Glenorchy event rheology and, given the contrast with the Judds Creek behaviour, should be considered as representing worst case scenarios because of its greater runout extent.

In each catchment, a place for the modelled debris flow to initiate (a source point) was placed in a gully head location where channelised debris flows might be expected to occur. A simplistic discharge vs time file was attached to each source point to supply the specified volume over an arbitrary 60 second interval. In setting up the model, the mesh was constructed in such a manner that the triangles in the source area were coarser than in the channel. As RF-2D writes the source file information to the triangle that it overlies, this tends to minimise any unrealistic lateral movement (across slope) if the discharge rate is too quick. Experiments were also performed with multiple source points clustered together (but overlying neighbouring mesh elements) for a given event where the total volume discharged is distributed evenly between points in order to minimise the lateral movement. However, while this approach can produce a better looking result in the source area, it makes little difference once the flow reaches the channel and for the sake of simplicity a single discharge point was adopted in all our simulations.

RF-2D provides a number of output formats including maximum depth, maximum velocity and hazard intensity. For the purposes of illustrating the results in this report, the Swiss Debris Flow schema (described in Lateltin, et al., 2005) is used (Figure 38).

The schema is based on 4 intensity classes (as seen on the legend), High, Medium, Low and None that are defined in the table below. However the Low class is not calculated by RF-2D as this is based on expected sedimentation values that currently cannot be calculated in the software. Despite this limitation, the method is useful as it provides a methodology for creating hazard maps and determining societal processes that follow, such as emergency management, land use planning and construction controls.

All other outputs, such as those that may be useful for designing mitigation structures, are provided in a data package to accompany this report.

Runout simulations are presented in the figures below (Figures 39, 40, 41, 42). Based on the assumptions previously described, it is evident that events of probability 1:500 or rarer begin to impact on the built environment. These simulations thus provide an indication of where attention can be focused to assess whether they pose risk to people and infrastructure.

Table 5. Design event volumes.

Catchments		Humphreys	New Town	Hobart	Browns	Total Study Area
Susceptible Area (km^3)		2.26	1.39	2.75	1.25	66.32
Event Probability (years)	100	18 000 m^3	10 000 m^3	20 000 m^3	9 000 m^3	
	500	80 000 m^3	50 000 m^3	100 000 m^3	40 000 m^3	
	1 000	180 000 m^3	100 000 m^3	200 000 m^3	80 000 m^3	
	2 000	250 000 m^3	200 000 m^3	300 000 m^3	180 000 m^3	

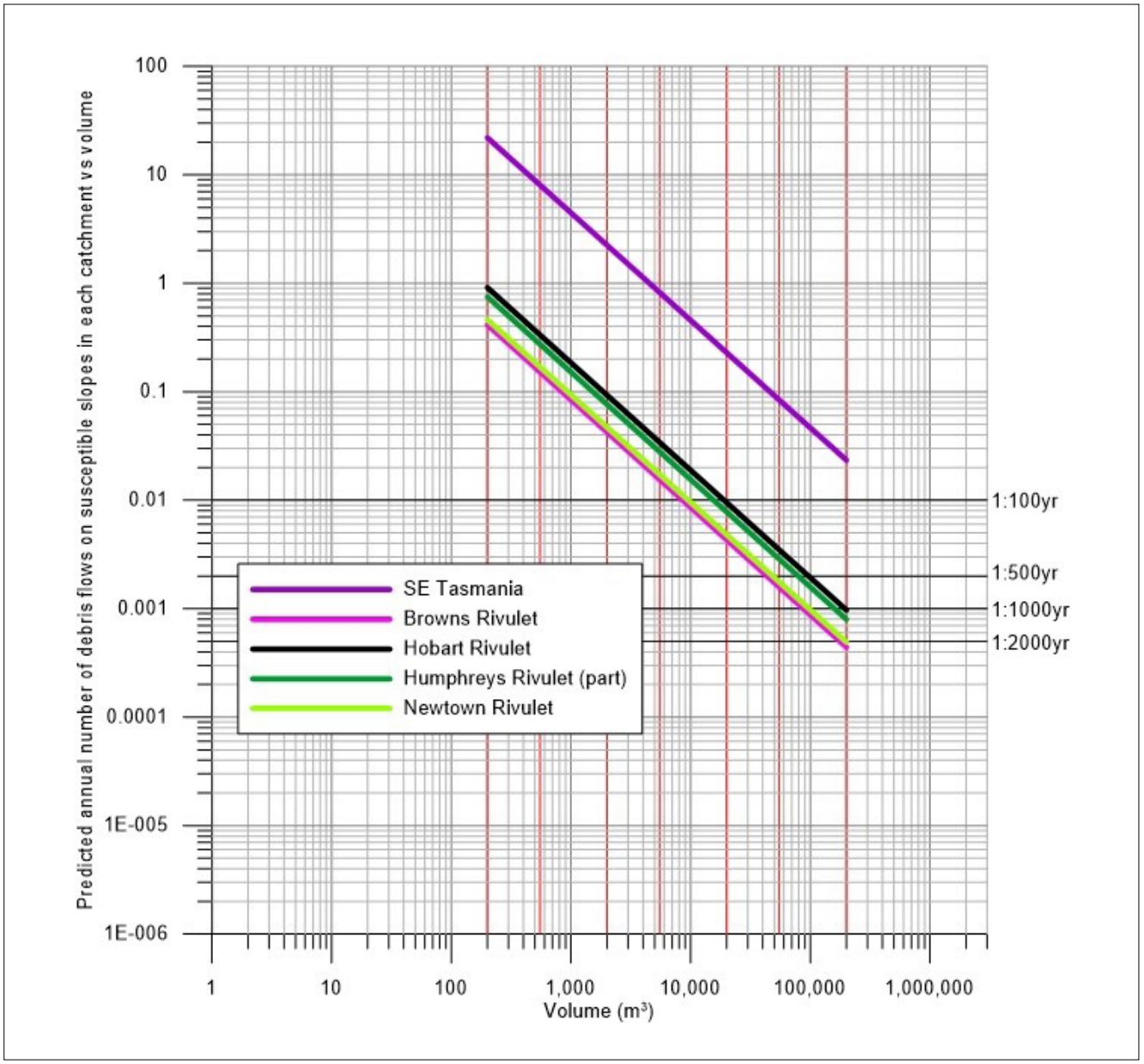

Figure 37. Probability distribution curves used for runout simulation.

Table 6. Swiss intensity definitions (Lateltin, et al., 2005). Note that RF-2D does not model the depth of soil material for potential debris flows therefore a low classification is not calculated.

Process	Intensity		
	Low	Medium	High
Rock falls			
Kinetic energy	<30 kJ	30 - 300kJ	>300kJ
Slides			
Mean annual velocity	<2 cm/year	2 -10 cm/year	>0.1 m/day
Displacement	-	-	>1 m/event
Debris flow			
Debris front thickness	-	<1 m	>1 m
Debris flow velocity	-	<1 m	>1 m/s
Depth of soil material (potential debris flows)	0.5 m	0.5 - 2 m	>2 m

Figure 38. 1:100 year probability runout simulations with the Swiss Debris Flow schema (red = high, blue = medium).

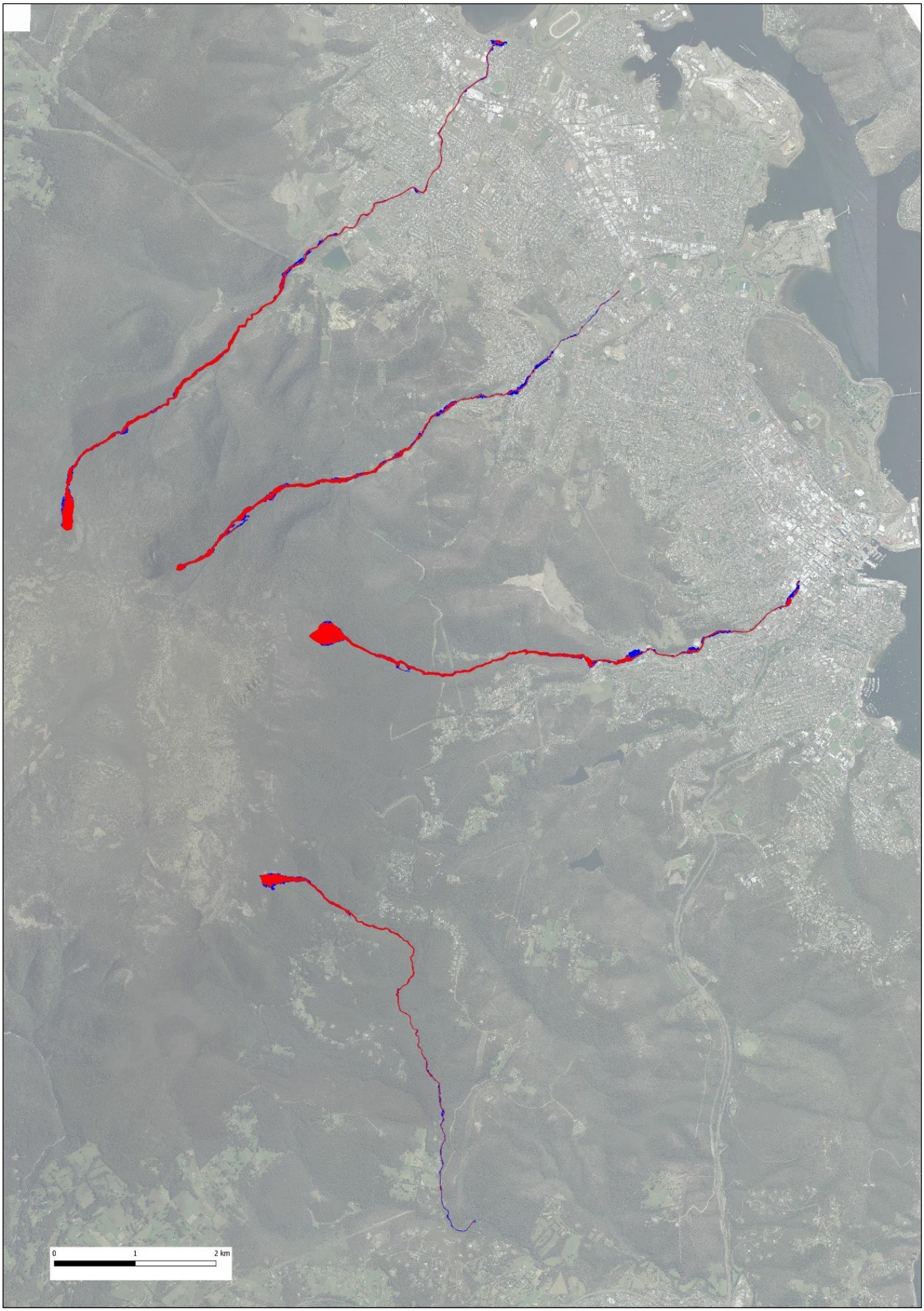

Figure 39. 1:500 year probability runout simulations with the Swiss Debris Flow schema (red = high, blue = medium).

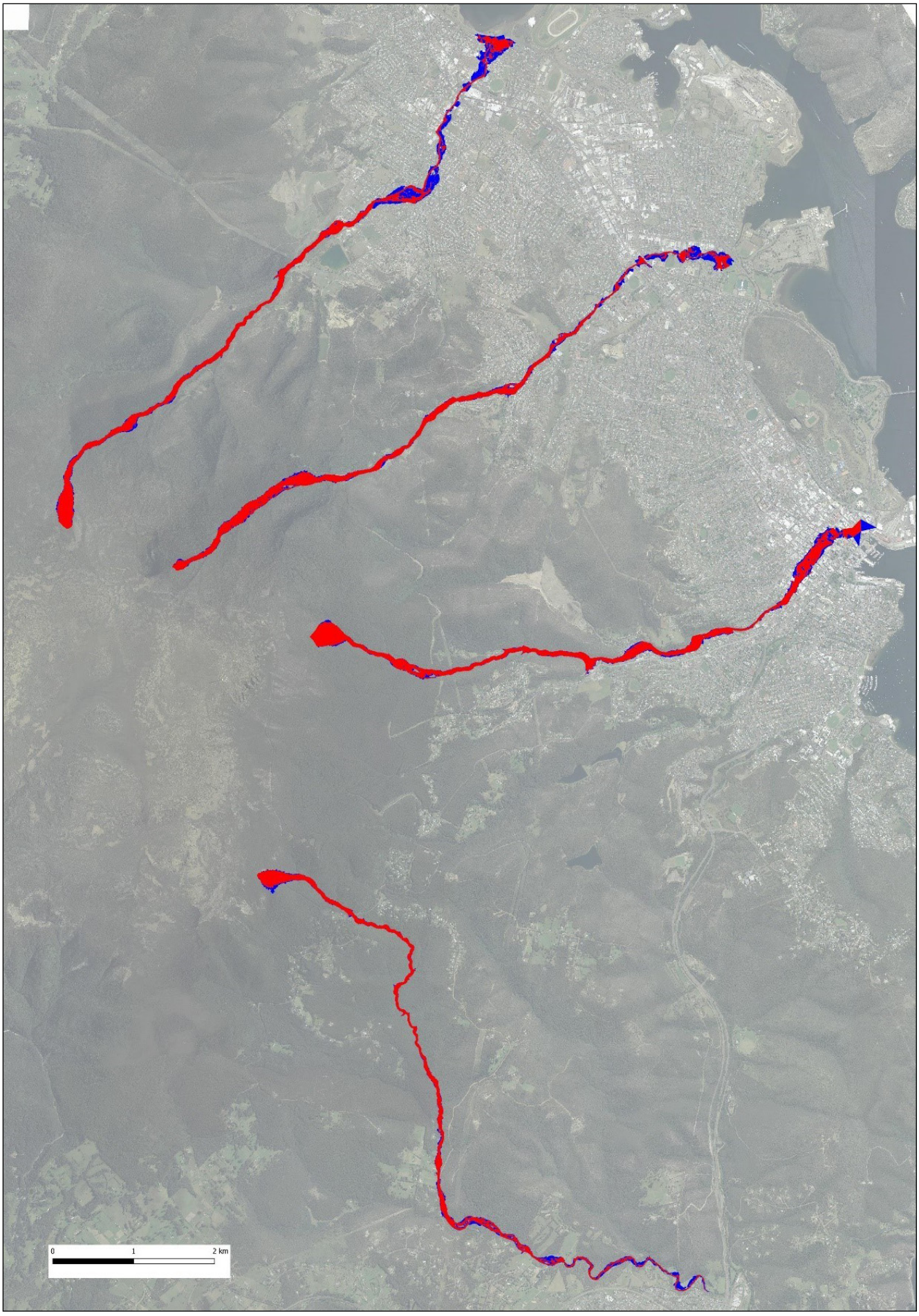

Figure 40. 1:1 000 year probability runout simulations with the Swiss Debris Flow schema (red = high, blue = medium).

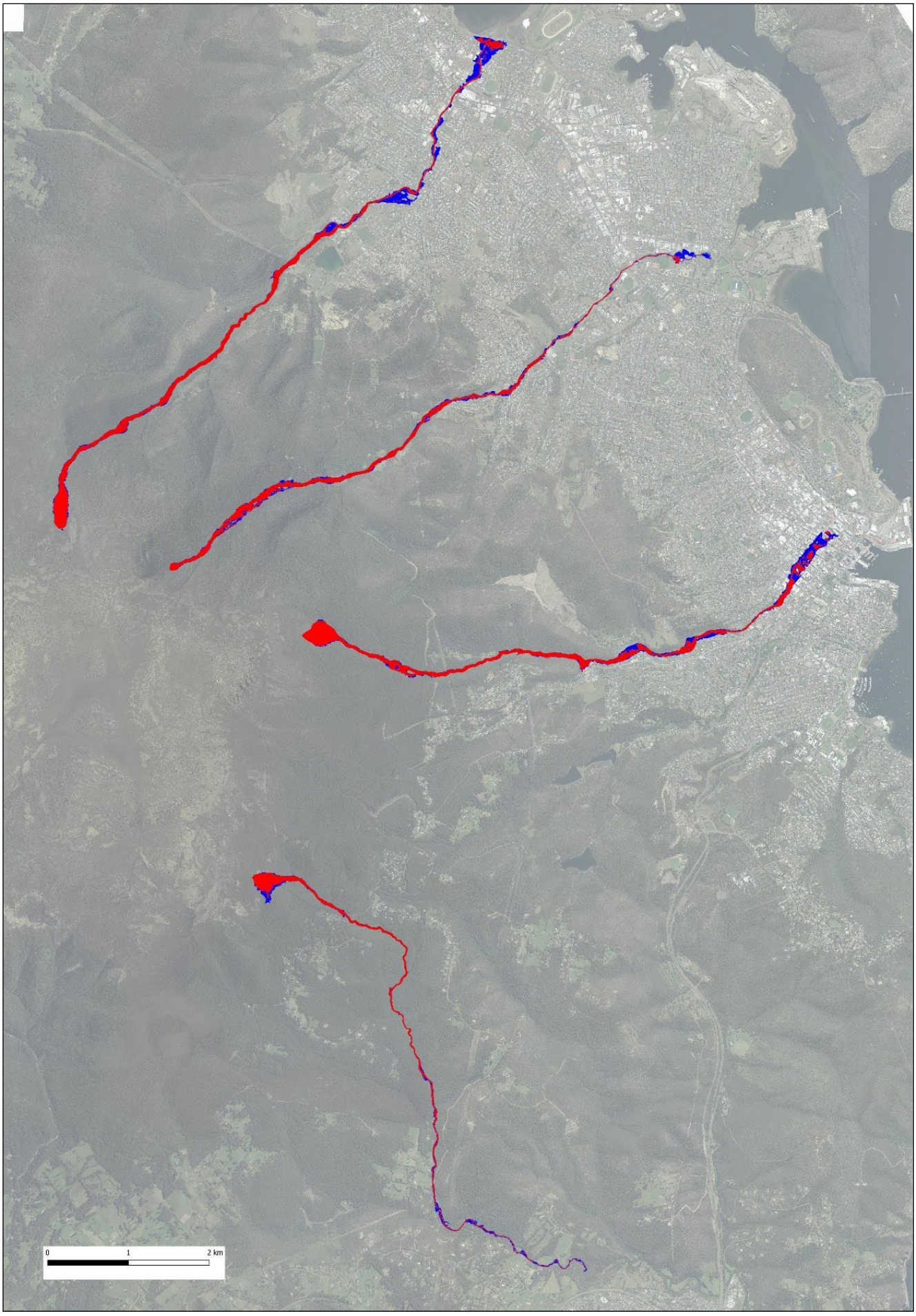

Figure 41. 1:2 000 year probability runout simulations with the Swiss Debris Flow schema (red = high, blue = medium).

6.0 CONCLUSION

A debris flow hazard assessment of kunanyi / Mount Wellington has been undertaken to provide information to assist stakeholders manage risk from future debris flow events. The assessment has involved a review of the geological mapping and geomorphic processes operating on the mountain; compilation and analysis of a regional debris flow dataset; quantification of geomorphic process rates; and regional susceptibility and design-event runout simulations using specialised software.

Based on several lines of evidence, we have presented models that, contrary to Fell and Moon (2007), do not involve an intermediate debris dam stage condition for the 1872 Glenorchy Debris Flow. This has important implications as if our model is correct, then the additional probability condition invoked by Fell and Moon is not required, and the probabilities of debris flows impacting in the lowland is consequently higher in our study.

Our modeling is based on a number of underlying assumptions that simplify what is a complex process. The simulations presented here utilise a rheology calibrated against the 1872 event that produces long run-out extents. This rheology condition can be regarded as a worst-case scenario on the basis of affecting more properties than a more viscous flow of similar volume.

The results of our study suggest that debris flows are a credible hazard to areas adjacent to the major waterways at the foot of the mountain (especially Humphreys, New Town and Hobart rivulets). Larger events may impact on developed areas of Hobart and Glenorchy down to the Derwent Estuary, as has happened in the past, if certain conditions are met and would have significant implications to infrastructure, buildings and people if realised. It should be noted that any existing structural mitigation measures that may be in place, but are not reflected in the DEM, have not been considered.

This report provides an understanding of the debris flow hazard emanating from key catchments on the mountain that can be used as a basis for developing appropriate risk-management strategies.

7.0 REFERENCES

AGS 2007a. Guideline for landslide susceptibility, hazard and risk zoning for land use planning. Australian Geomechanics Society, *Australian Geomechanics*, 42(1): 13-36 [available online: www.australiangeomechanics.org].

AGS 2007b. Commentary on guideline for landslide susceptibility, hazard and risk zoning for land use planning. Australian Geomechanics Society, *Australian Geomechanics*, 42(1): 37-58 [available online: www.australiangeomechanics.org].

Anon. 2016. *Wellington Park featuring kunanyi / Mt Wellington. Recreation map and notes.* TASMAP. Land Tasmania, Department of Primary Industries, Parks, Water and Environment: Hobart.

Barrows, T. T., Stone, J. O. and Fifield, L. K. 2004. Exposure ages for Pleistocene periglacial deposits in Australia. *Quaternary Science Reviews,* 23: 697-708.

Brunetti, M. T., Guzzetti, F. and Rossi, M. 2009. Probability distributions of landslide volumes. *Nonlinear Processes in Geophysics,* 16: 179–188.

Cannon, S. H. and Gartner, J.E. 2005. Chapter 15: Wildfire-related debris flow from a hazards perspective. In: Jakob, M; Hungr, O (eds). Debris-flow Hazards and Related Phenomena, Springer-Verlag, Berlin, Praxis, 363-385.

Colhoun, E. A. 2002. Periglacial landforms and deposits of Tasmania. *South African Journal of Science*, 98: 55-63.

Corbett, K. D., Quilty, P. G. and Calver, C. R. (eds) 2014. Geological Evolution of Tasmania. *Geological Society of Australia special publication*, 24 .

Corominas, J. 1996. The angle of reach as a mobility index for small and large landslides. *Canadian Geotechnical Journal*, 33: 260-271.

Cruden, D. M. and Varnes, D. J. 1996. Landslide types and processes. In: Turner, A.K.; Schuster, R.L. (eds), *Landslides: investigation and mitigation*. Transportation Research Board (National Research Council) Special Report 247. National Academy Press: Washington, D.C. 36-75.

Davies, J. L. 1958. The cryoplanation of Mt. Wellington. *Papers and Proceedings of the Royal Society of Tasmania,* 92: 151-154.

Davies, T. R. H., Phillips, C. J., Pearce, A. J. and Zhang, X. B. 1992. *Debris flow behaviour — an integrated overview. Erosion, Debris Flows and Environment in Mountain Regions (Proceedings of the Chengdu Symposium, July 1992*, Chengdu, China, vol. 209. IAHS.

Dietrich, W. E. and Montgomery, D. R. 1998. SHALSTAB: a digital terrain model for mapping shallow landslide potential, NCASI Technical Report [available online: http://calm.geo.berkeley.edu/geomorph/shalstab/index.htm].

Dowling, C. A. and Santi, P. M. 2014. Debris flows and their toll on human life: a global analysis of debris-flow fatalities from 1950 to 2011. *Natural Hazards,* 71(1): 203-227.

Fell, R. and Moon, A. T. 2007. *Final report on the review of Mineral Resources Tasmania landslide hazard zoning, Mt. Wellington-Hobart area debris flows. Report to Hobart Water*, by UNSW Global Consulting and Coffey Geotechnics: Sydney. 38p. [available online: www.ses.tas.gov.au].

Forsyth, S. M., Quilty, P. G. and Calver, C. R. 2014. Cenozoic onshore basins and landscape evolution. In: Corbett, K.D.; Quilty, P.G.; Calver, C.R. (eds), Geological evolution of Tasmania, vol. *Geological Society of Australia special publication,* 24. Geological Society of Australia (Tasmania Division). 437-452.

Guzzetti, F. 2005. *Landslide hazard and risk assessment*. PhD thesis, University of Bonn: Bonn, Germany.

Hofto, P. J., Sloane, D. J. and Weldon, B. D. 1991. Engineering geology of the greater Hobart area. Division of Mines and Mineral Resources, Tasmania, *Urban Geological Mapping Project Report*, 1. 62p. [available online: www.mrt.tas.gov.au].

Horton, P.; Jaboyedoff, M.; Rudaz, B. and Zimmermann, M. 2013. Flow-R, a model for susceptibility mapping of debris flows and other gravitational hazards at a regional scale. *Natural Hazards and Earth System Science*: 869-885.

Hovius, N., Stark, C. P. and Allen, P. A. 1997. Sediment flux from a mountain belt derived by landslide mapping. *Geology*, 25: 231–234.

Hunter, G. and Fell, R. 2002. Estimation of travel distance for landslides in soil slopes. *Australian Geomechanics,* 37(2): 65-82.

IAEG International Commission on Landslides 1990. Suggested nomenclature for landslides. *Bulletin of the International Association of Engineering Geology,* 41: 13-16.

Iverson, R. M. 2003. The debris-flow rheology myth. In: Rickenmann, D.; Chen, C.-L. (eds), Debris-Flow Hazards Mitigation: Mechanics, *Prediction, and Assessment*, 1. Millpress: Rotterdam. pp.303-314.

Klar, A., Aharonov, E., Kalderon-Asael, B. and Katz, O. 2011. Analytical and observational relations between landslide volume and surface area. *Journal of Geophysical Research: Earth Surface,* 116(F2): F02001

Lateltin, O., Haemmig, C., Raetzo, H. and Bonnard, C. 2005. Landslide risk management in Switzerland. *Landslides,* 2: 313-320.

Leaman, D.E. 1976. Geological Survey Explanatory Report, Geological atlas 1:50000 Series, Sheet 82 (83125) *Hobart*. Department of Mines: Hobart.

Malamud, B.D.; Turcotte, D.L.; Guzzetti, F.; Reichenbach, P. 2004. Landslide inventories and their statistical properties. John Wiley & Sons, Ltd., *Earth Surface Processes and Landforms,* 29(6): 687-711 [available online: http://dx.doi.org/10.1002/esp.1064].

Mazengarb, C. 2004a. Glenorchy, map 3 - Potential debris-flow hazard. Tasmanian Landslide Hazard Series (1:25 000). Mineral Resources Tasmania, Department of Infrastructure Energy and Resources: Hobart [available online: www.mrt.tas.gov.au].

Mazengarb, C. 2004b. Hobart, map 3 - Potential debris-flow hazard. *Tasmanian Landslide Hazard Series* (1:25 000). Mineral Resources Tasmania, Department of Infrastructure Energy and Resources: Hobart [available online: www.mrt.tas.gov.au].

Mazengarb, C. 2005. The Tasmanian landslide hazard map series: methodology. *Tasmanian Geological Survey Record,* 2005/04. Mineral Resources Tasmania. 43. [available online: www.mrt.tas.gov.au].

Moon, A.T.; Olds, R.J.; Wilson, R.A.; Burman, B.C. 1992. Debris flow zoning at Montrose, Victoria In: BELL, D.H. (ed.), *Proceedings of the sixth international symposium on landslides,* Christchurch, New Zealand, 2. A.A. Balkema: Rotterdam,The Netherlands. 1015-1022.

Moon, A.T.; Wilson, R.; Flentje, P.N. 2005. Developing and using landslide size frequency models. In: Hungr, O.; Fell, R.; Couture, R. (eds), *Landslide risk management*. Eberhardt, Taylor and Francis: London. 680-690.

Naef, D.; Rickenmann, D.; Rutschmann, P.; Mcardell, B.W. 2006. Comparison of flow resistance relations for debris flows using a one-dimensional finite element simulation model, *Natural Hazards and Earth System Science,* 6(1): 155-165.

O'Brien, J.S.; Julien, P.Y. 1988. Laboratory analysis of mudflow properties. *Journal of Hydraulic Engineering*, 114(8): 877-887.

Pack, R.T.; Tarboton, D.G.; Goodwin, C.N.; Prasad, A. 2005. SINMAP 2. *A Stability Index Approach to Terrain Stability Hazard Mapping, technical description and users guide for version 2.0*. Utah State University.

Pierson, T.C. 2005a. Distinguishing between debris flows and floods from field evidence in small watersheds, Fact Sheet. Report. Report No: 2004-3142. 4p. [available online: http://pubs.er.usgs.gov/publication/fs20043142].

Pierson, T.C. 2005b. Hyperconcentrated flow – transitional process between water flow and debris flow. In: JAKOB, M.; HUNGR, O. (eds), *Debris-Flow Hazards and Related Phenomena*. Springer: Berlin. 159–202.

Pierson, T.C.; Costa, J.C. (eds) 1987. A rheologic classification of subaerial sediment-water flows. in Costa J. E.; Wieczorek g. f. (eds), Debris flows/avalanches: process, recognition and mitigation, *Geological Society of America Reviews in Engineering Geology,* 7: 1–12.

Prochaska, A.B.; Santi, P.M.; Higgins, J.D.; Cannon, S.H. 2008. A study of methods to estimate debris flow velocity. *Landslides,* 5(4): 431-444.

Rickenmann, D. 1999. Empirical relationships for debris flows. *Natural Hazards,* 19: 47-77 [available online: http://www.scopus.com/scopus/inward/record.url?eid=2-s2.0-0032711715&partnerID=40&rel=R5.6.0].

Rickenmann, D. 2005. Runout prediction methods. In: *Debris-flow Hazards and Related Phenomena*, Chapter 13. Springer Praxis Books. Springer Berlin Heidelberg. pp.305-324 [available online: http://dx.doi.org/10.1007/3-540-27129-5_13].

Rickenmann, D. 2016. Debris-Flow Hazard Assessment and Methods Applied in Engineering Practice. *International Journal of Erosion Control Engineering,* 9(3).

Rutherfurd, I.D.; Bishop, P.; Loffler, T. 1994. Debris flows in northeastern Victoria, Australia: occurrence and effects on the fluvial system. Variability in stream erosion and sediment transport,

Proceeding of the Canberra Symposium December 1994, 224, 359-369.

Stevenson, M.D.; Woolley, R.N.; Mazengarb, C. 2016. Historical assessment of the 1872 Glenorchy debris flow: a basis for modelling the large debris flow hazard from the Wellington Range, Hobart, Unpublished Report 2016/02. 106.

Stevenson, P.C. 1980. The deterioration of a dolerite escarpment. *Third Australia-New Zealand Conference on Geomechanics*, Wellington, New Zealand, May 12-16, 1980, vol. 2. Proceedings of Technical Groups 6(1). New Zealand Institution of Engineers, 87-91.

Takahashi, T. 2007. Progress in Debris Flow Modeling. In: Sassa, K.; Fukuoka, H.; Wang, F.; Wang, G. (eds), *Progress in Landslide Science*, Chapter 5. Springer Berlin Heidelberg. 59-77.

Takahashi, T. 2014. *Debris Flow: Mechanics, Prediction and Countermeasures,* 2nd Edn. CRC Press: London, UK. 551.

Timilsina, M.; Bhandary, N.P.; Dahal, R.K.; Yatabe, R. 2014. Distribution probability of large-scale landslides in central Nepal. *Geomorphology,* 226: 236-248.

Wasson, R.J. 1977a. Catchment processes and evolution of alluvial fans in the lower Derwent Valley, Tasmania. *Zeitschrift für Geomorphologie,* 21: 147-168.

Wasson, R.J. 1977b. Last-glacial alluvial fan sedimentation in the lower Derwent Valley, Tasmania. *Sedimentology,* 24: 781-799.

Whipple, K.X.; Dunne, T. 1992. The influence of debris-flow rheology on fan morphology in Owens Valley, California. *Geological Society of America Bulletin*, 104: 887-900.

APPENDIX 1

Located :

https://www.mrt.tas.gov.au/mrtdoc/dominfo/download/TR37/

Appendix 1 - Geomorphology and simplified geology of kunanyi

-Download-

APPENDIX 2

Judds Creek debris flow (landslide 2441)

Judds Creek Debris Flow

The largest debris flow recognised in SE Tasmania occurs near Judds Creek in the Huon Catchment (landslide 2441 in our database) (Figure 43) and provides an opportunity to compare against a similar sized feature, the 1872 Glenorchy Debris Flow event previously described (Stevenson, et al., 2016). We have not found any historical records of this event and was only discovered in our review of the state aerial mapping catalogue.

Aerial photos (see below) were examined in stereo and orthophotos produced in order to understand the conditions prior to and after the landslide forming. In addition, LiDAR imagery also exists that has assisted our analysis.

The Judds Creek landslide initiated sometime between state aerial photography surveys in 1947 and 1965. During this time at least one major rainfall event occurred, in April 1960, associated with regional scale flooding (source: Bureau of Meteorology website) that may be the trigger for the landslide. The nearest rainfall record is about 20 km away in the New Norfolk area where over 250 mm of rain fell in less than 48 hours. The rainfall trigger hypothesis for this landslide is supported by a recollection by the father of one of our former colleagues at MRT (RN Woolley pers comm), who indicated that Judds Creek was affected by significant aggradation in the 1960 – 1961 timeframe.

According to the MRT 1:250 000 geological map, the landslide has formed within Tasmanian Dolerite Formation. However, given the flow style of the landslide, it is considered likely that the failed material was deeply weathered to soil strength properties and thus similar to the 1872 Glenorchy Debris Flow event. There is a suggestion that a large slump block exists adjacent to the landslide (see below) which if true, further supports the contention that the strength of the dolerite is much lower here.

A morphological interpretation of the pre-failure landscape based on the 1947 photos is provided (Figure 44). The photos were orthorectified and a digital surface model (DSM) created although the quality is poor and limited overlap meant that the accuracy of this was poor (Figure 45).

The landslide has formed on an escarpment below a local plateau and centred on a small unnamed tributary. The photos show evidence of recent forest clearance upstream of the landslide while the surrounding area is in pasture. The pasture is covered with many fallen logs indicating forest clearance by European settlers dates further back in time.

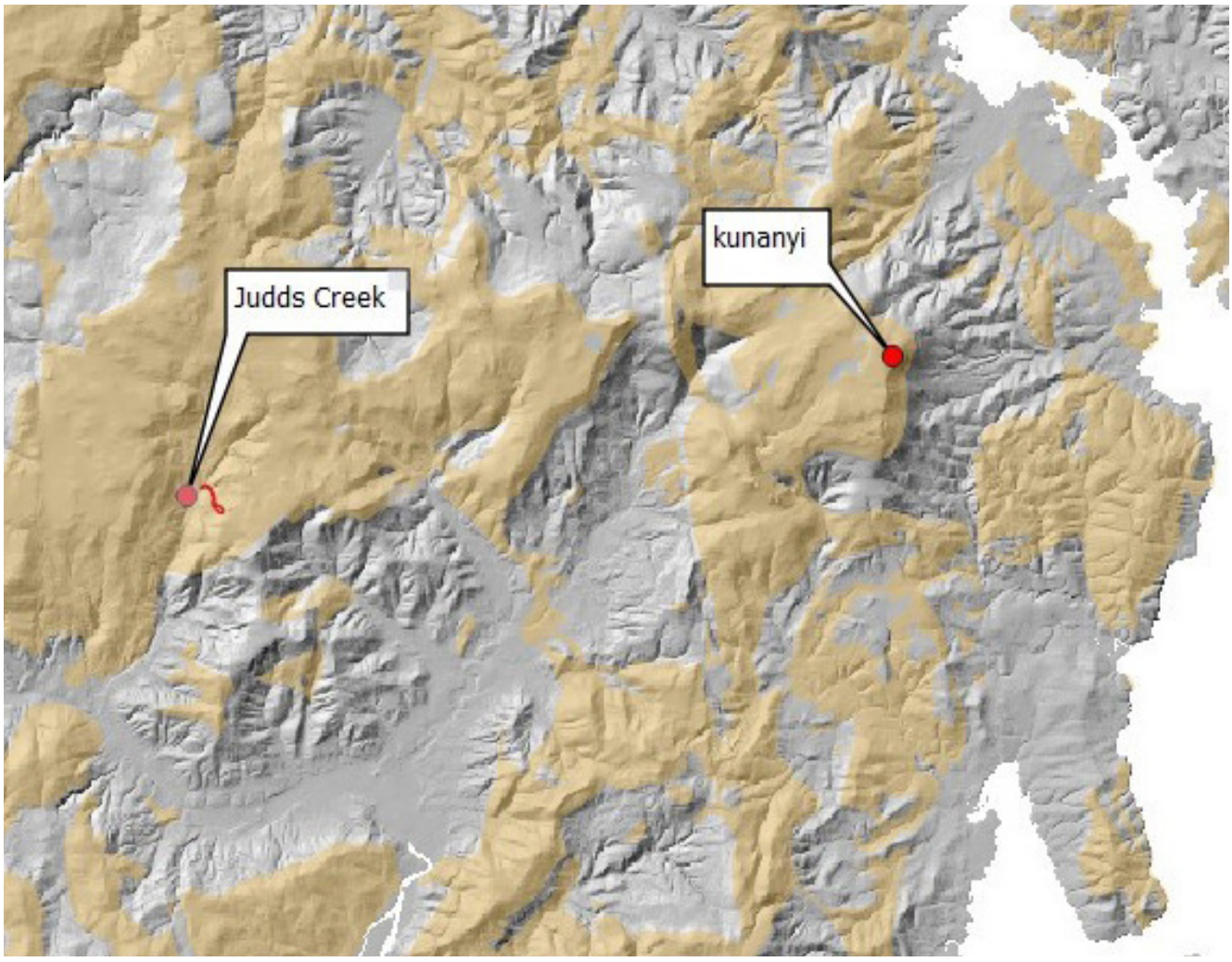

Figure 1. Location of landslide 2441 at Judds Creek, west of kunanyi. Brown overlay is area of Jurassic dolerite from the MRT 1:250k geology layer

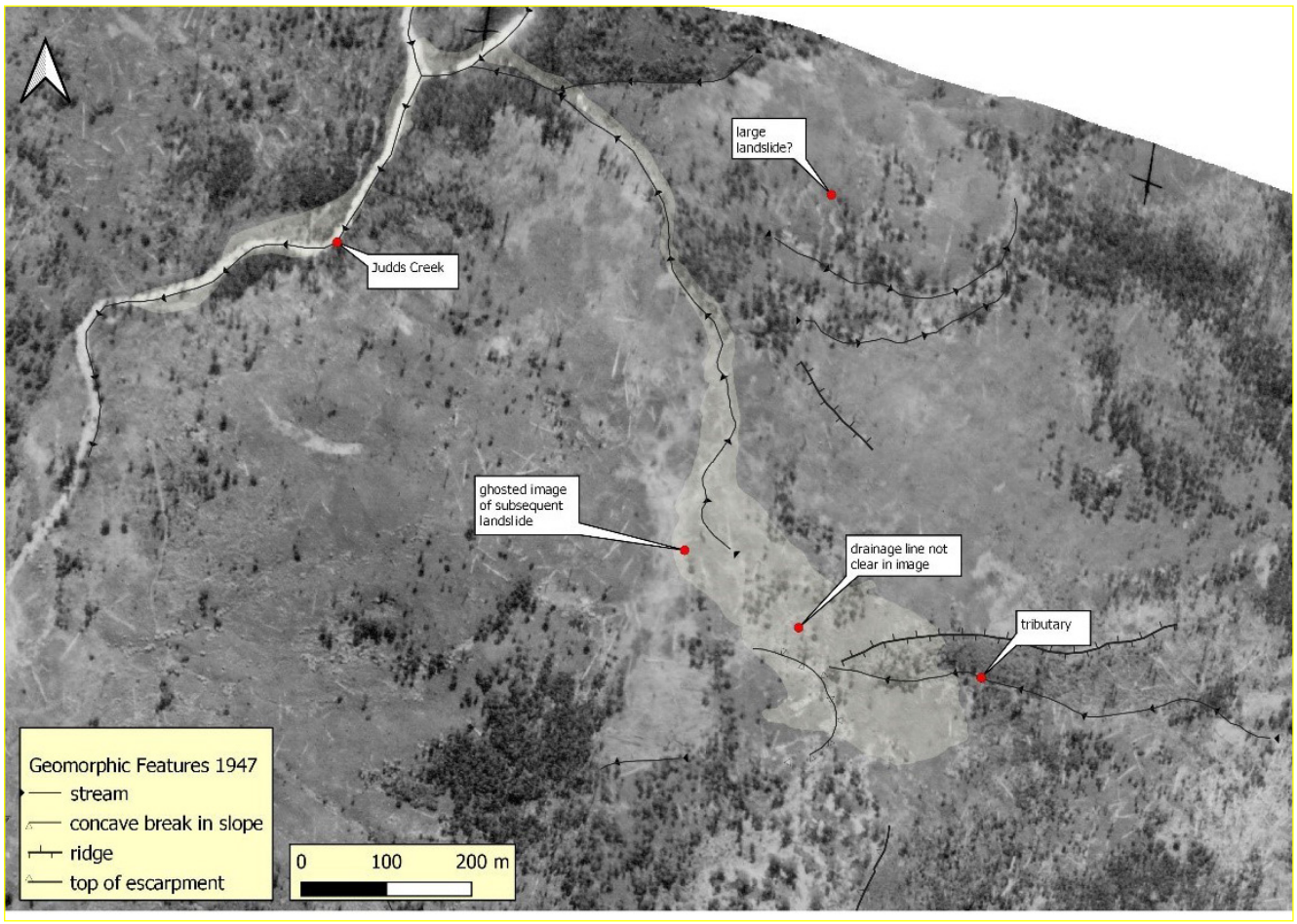

Figure 2. Orthorectified aerial photographs (1947_styx_24540-42) dated 27/2/1947 with area of subsequent landslide ghosted for reference.

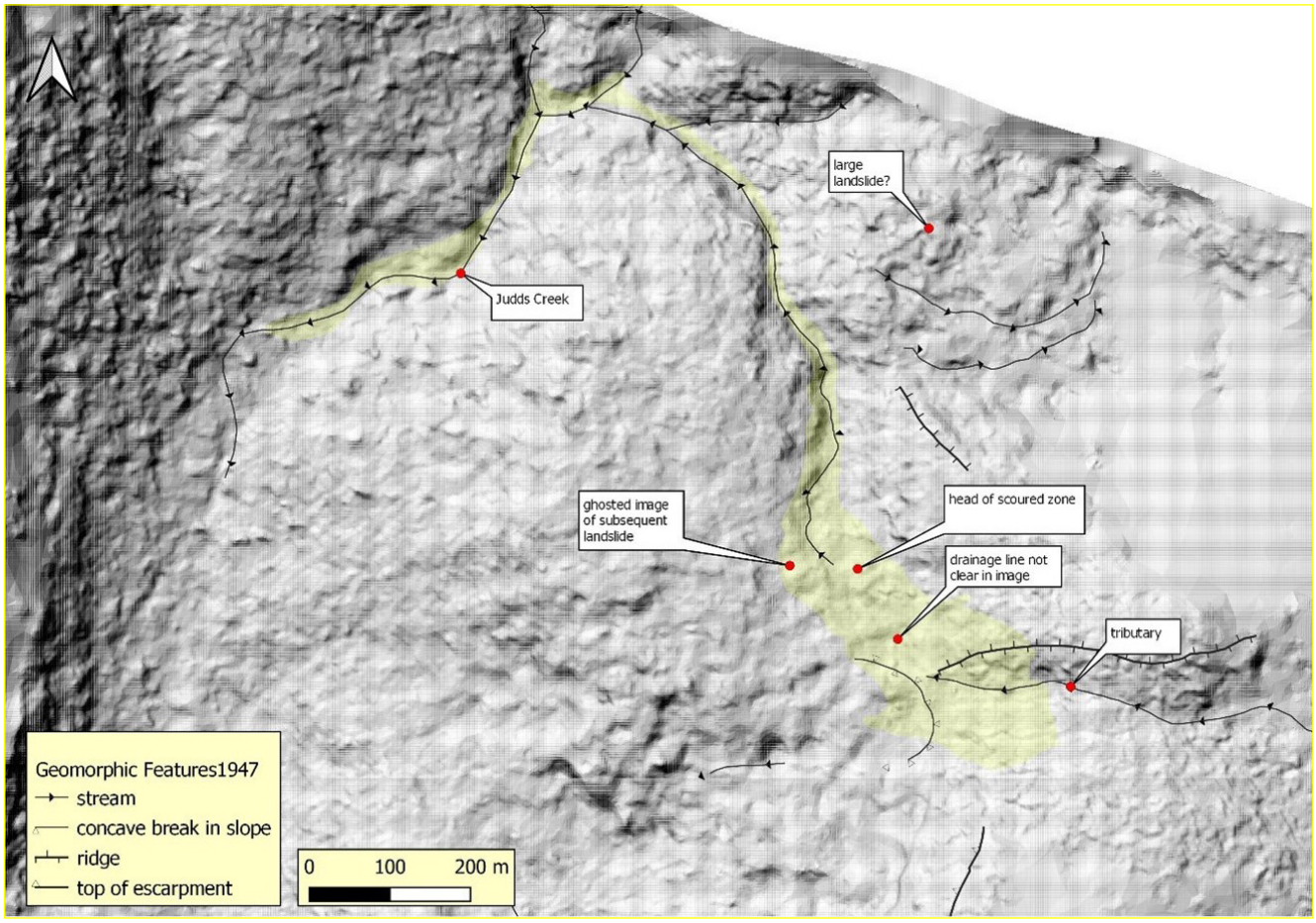

Figure 3. Hillshade based on a DSM generated from the 1947 images. Contours are not shown as they are unreliable.

The 1965 aerial photography in contrast is of much higher quality and shows a relatively fresh landslide morphology with limited revegetation. Later photos, 1975 onwards (and satellite images) show progressive revegetation with most of the landslide now almost completely overgrown. The 1965 photos were examined in stereo and were also used to create a georeferenced orthophoto. The quality of the photos allowed much detail to be recognised in stereo view that was transferred into GIS layers using the orthophoto as a base. The analysis also benefitted from publicly available LiDAR imagery captured in 2013 that provided an accurate digital elevation model on which to constrain the orthophotos (Figures 4, 5, 6 and 7).

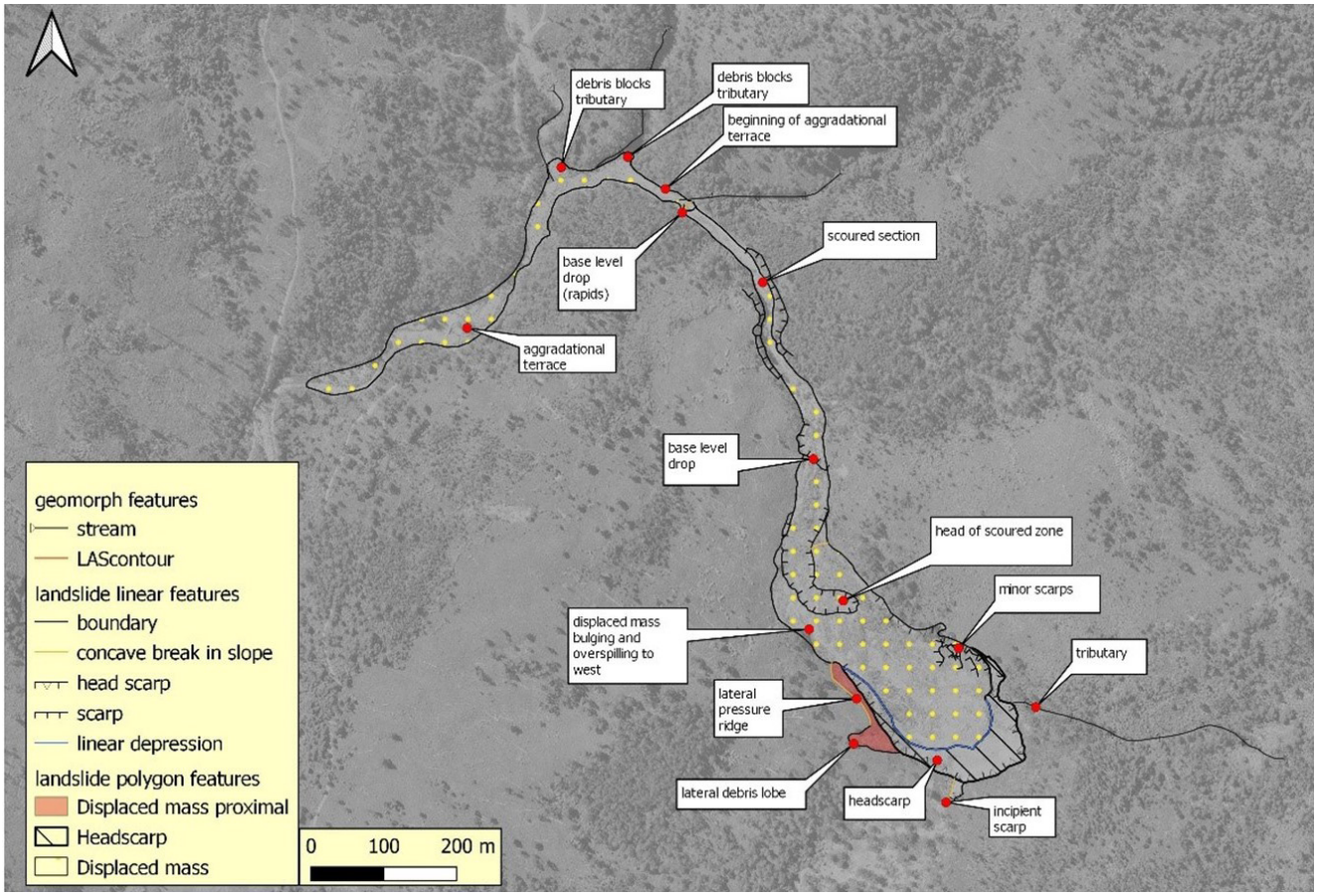

Figure 4 (above). Orthorectified aerial photographs (0444_258-60) dated 17/2/1965, showing features of the landslide.

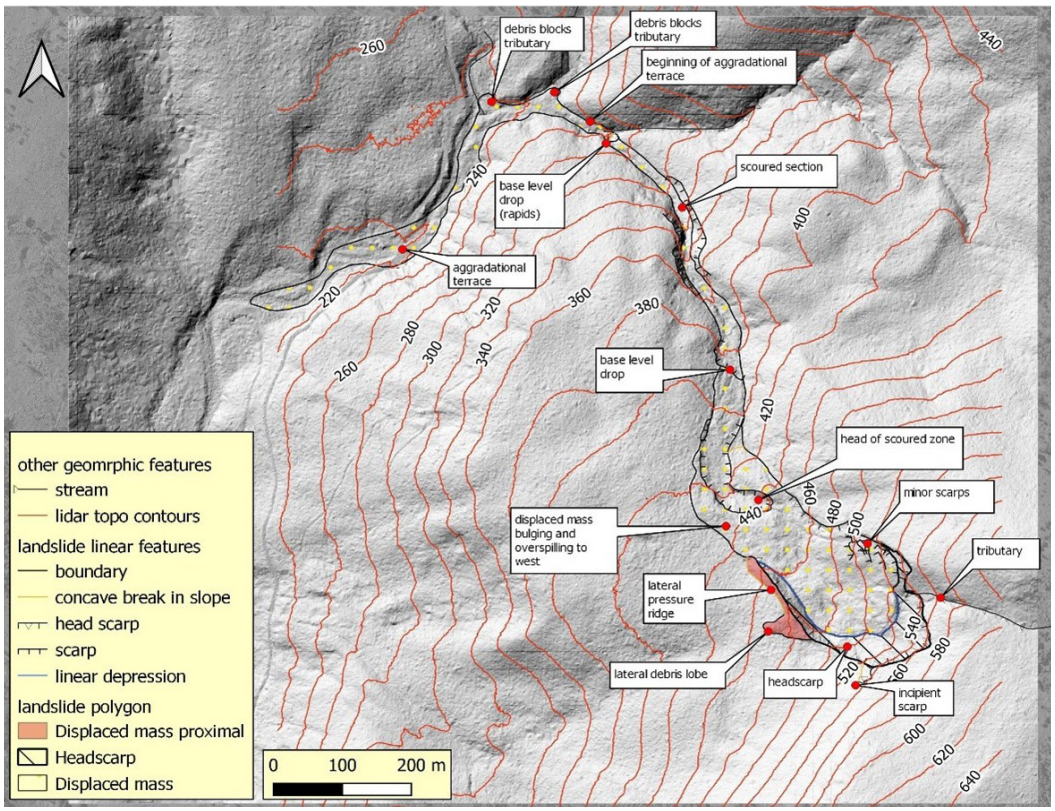

Figure 47 (left). 1965 orthophoto with LiDAR derived hillshade and contours.

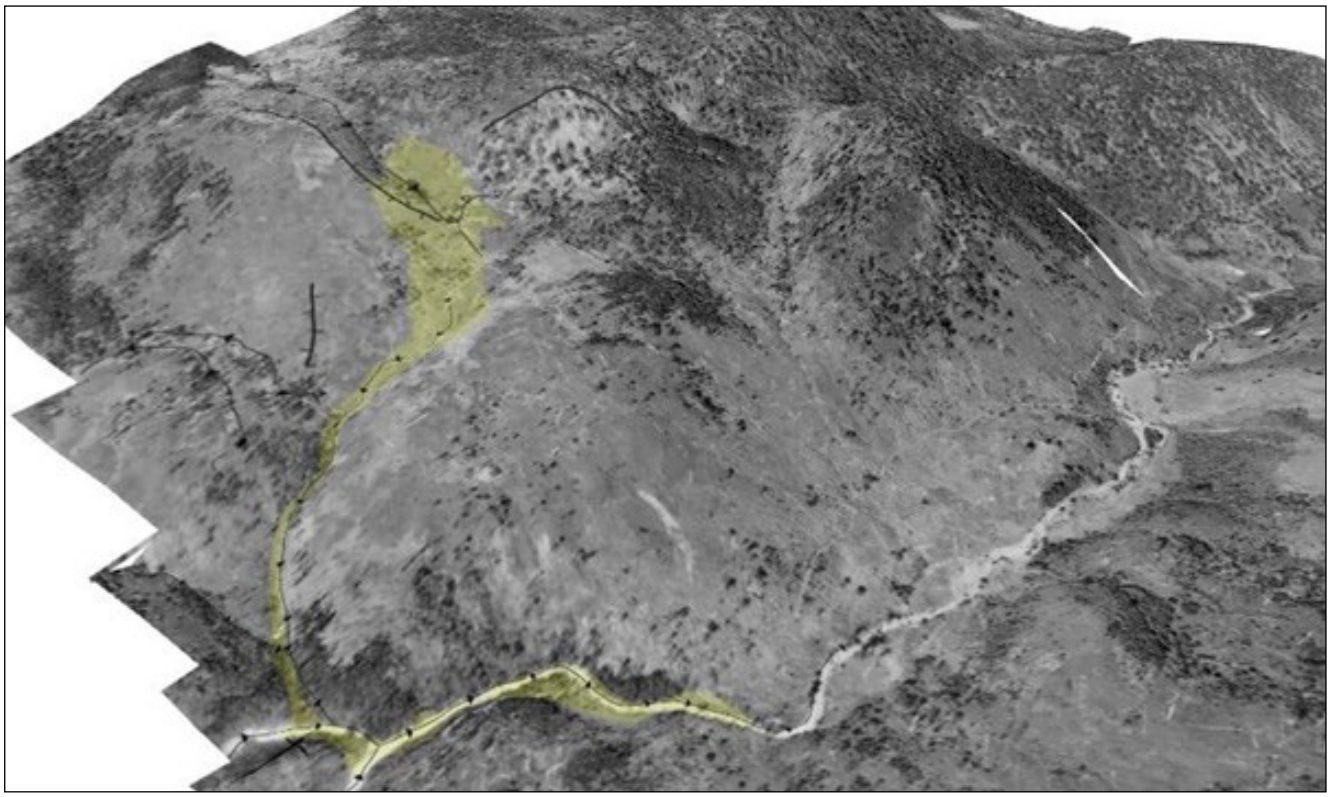

Figure 48. Oblique image of 1947 aerial photographs draped over a DSM constructed from these photos with area of subsequent landslide indicated.

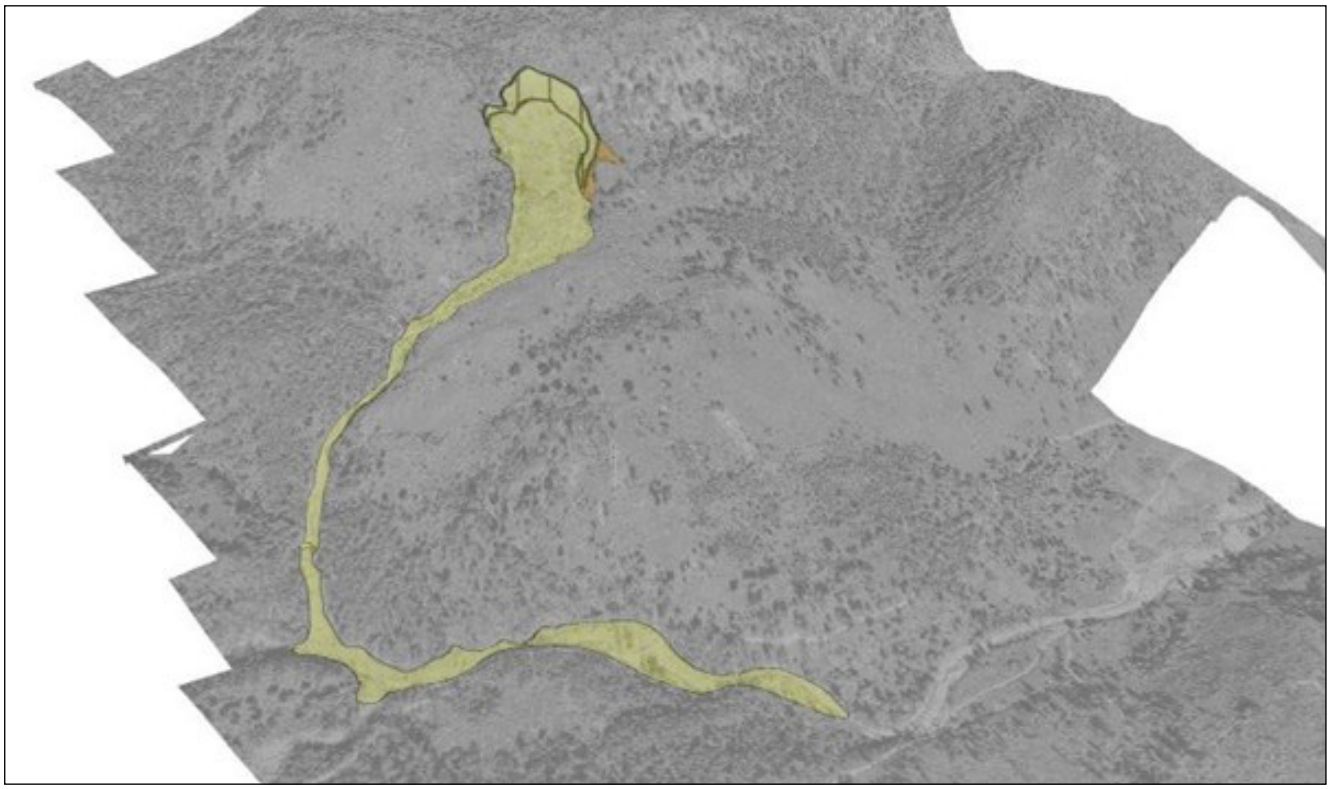

Figure 49. Oblique image constructed using Structure from Motion software on 1965 aerial photographs.

Based on our remote sensing interpretation, it is suggested that the landslide has two major components, hereby referred to as the upper and lower parts:

- The upper part, from the headscarp down to about the 400 m contour contains the majority of the displaced mass. A precise volume estimation is difficult as the position of the foot and the depth of rupture have uncertainties that would require subsurface investigation to elucidate. In this exercise a half ellipsoid geometry calculation is chosen (as described in Cruden and Varnes, 1996) and, depending on the input parameters, ranges between 300 000 to 500 000 m^3. A value of 400 000 m^3 is adopted in this study. It is estimated that the tongue of this feature extends about 200 m beyond the foot.
- The lower part of the landslide is expressed as an incised (scoured) channel in its upper part and transitioning into an aggradational deposit lower down. It is considered that this is an expression of a debris flow that has formed as a secondary phase to the larger feature. Of the most compelling criteria for designating a debris flow mechanism (over a flood deposit) are the deposits damming two tributaries and containing mixtures of logs and coarse sediment. These deposits are likely to have been rapidly deposited overwhelming any flood waters coming from the much larger catchments drained by the tributaries. The volume of this phase is calculated from the dimensions of the channel and estimated to be about 20 000 m^3.

Tasmanian
Government

Mineral Resources Tasmania
PO Box 56 Rosny Park
Tasmania Australia 7018
Ph: +61 3 6165 4800

info@mrt.tas.gov.au www.mrt.tas.gov.au